

BEAM-BEAM INTERACTION WITH LONGITUDINAL IMPEDANCE AND ITS APPLICATION IN TMCI STUDY

Chuntao Lin*, Institute of Advanced Science Facilities, Shenzhen, Guangdong, 518107, China
Kazuhito Ohmi, KEK, Tsukuba, Ibaraki 305-0801, Japan
Yuan Zhang, Institute of High Energy Physics, Beijing 100049, China

Abstract

Simulations have showed a novel coherent head-tail instability induced by beam-beam interaction with a large Piwinski angle. The localized cross-wake force has been introduced to explain the instability. The longitudinal impedance would cause coherent and incoherent synchrotron tune shift and distort the particle's trajectories in longitudinal phase space. Further beam-beam simulation revealed that the longitudinal impedance has strong impacts on the beam stability, squeezing the horizontal stable tune area seriously. The instability has become an important issue during the designs of CEPC and FCC-ee. In this paper, we develop a transverse mode coupling analysis method that could be used to study beam-beam instability with and without longitudinal impedance. This method can also be applied in synchrotron light sources to study transverse mode coupling instability (TMCI) with longitudinal impedance and harmonic cavity. Some preliminary results at Shenzhen Innovation Light Source (SILF) are also shown.

INTRODUCTION

Beam-beam interaction with a crossing angle has been studied for many years. Usually, it is believed that the horizontal oscillation of colliding bunch would be very stable. However, during the study of FCC-ee, the simulations [1] showed that there exists a coherent head-tail instability (X-Z instability) in collision with a large Piwinski angle. The "cross-wake force" induced by beam-beam interaction has been introduced to successfully explain this newfound instability [2, 3].

The stability of horizontal motion is sensitive to the longitudinal dynamics. The longitudinal impedance would modify the beam distribution, distort the longitudinal phase space trajectory, and produce incoherent synchrotron tune shift. Strong-strong simulation [4] showed that the stable tune area would be shifted, and the width would be squeezed when the longitudinal impedance is included in the simulation. It is interesting to study how the longitudinal impedance influences the X-Z instability analytically.

The ordinary transverse mode coupling instability (TMCI) theory [5] is derived as a perturbed Vlasov equation. In this theory, the transverse impedance, a perturbation source, represents the averaged wake force around the circumference of the ring. The TMCI is based on the solution of Sacherer's integral equation, only a few analytic solutions are known for some specific beam distributions so far. Some transverse

mode coupling analytical methods have been developed to treat the localized wake force [2, 3]. However, the distortion of longitudinal phase space trajectory and the incoherent synchrotron tune shift were not considered in these papers. In this paper, we will develop a new transverse mode coupling method where the effects of longitudinal phase space trajectory distortion and incoherent synchrotron tune shift induced by longitudinal impedance could be considered.

LONGITUDINAL MOTION WITH WAKEFIELD

We use $s = z + v_0 t$ with s the longitudinal Serret-Frenet coordinate, representing the arc length measured along the closed orbit from an initial point, $v_0 \approx c$ the synchronous velocity and t clock time. z is the longitudinal distance from the synchronous particle and $z > 0$ is the bunch head. In the following, we will use s as the timelike variable and z as the longitudinal coordinate.

As the particle moves along the beamline, the head of the bunch will act as a source of an electromagnetic field that kicks the tail. In one revolution, the relative longitudinal momentum kick $\Delta\delta(z)$ received by a particle at z can be expressed by a wake function [5],

$$\Delta\delta(z) = -\frac{N_0 r_e}{\gamma} \int_{-\infty}^{\infty} W_z(z-z') \rho(z') dz'. \quad (1)$$

$W_z(z)$ is the ordinary longitudinal wake function with the property $W_z(z) = 0$ ($z > 0$). N_0 represents the single bunch population, r_e is the classical radius of the electron, γ is the relativistic factor and $\rho(z)$ is normalized line density.

Including the longitudinal wakefield, the Hamiltonian of the particle then reads,

$$-H = \frac{\eta_p}{2} \delta^2 + \frac{\mu_z^2}{2\eta_p L^2} z^2 - \frac{1}{L} \frac{N_0 r_e}{\gamma} \int_0^z dz'' \int_{-\infty}^{\infty} dz' W_z(z''-z') \rho(z') \quad (2)$$

where L represents the circumference of the ring, ν_s is the synchrotron tune, $\mu_z = 2\pi\nu_s$, η_p is the slippage factor.

For electron machine, due to the synchrotron radiation, the stationary distribution should have a Gaussian distribution with the RMS value σ_δ in δ ,

$$\psi(z, \delta) = \frac{1}{\sqrt{2\pi}\sigma_\delta} \exp\left(-\frac{\delta^2}{2\sigma_\delta^2}\right) \rho(z). \quad (3)$$

$\rho(z)$ can be obtained by solving Haissinski equation.

* linctao@yeah.net

RESEARCH ON BEAM DYNAMICS OF A 2 GeV 6 MW ISOCHRONOUS FFA*

Tianjue Zhang[†], Wei Fu¹, Chuan Wang¹, Tianjian Bian¹, Shilun Pei¹, Zhiguo Yin¹, Hongji Zhou¹,
 Ziye Yin², Suping Zhang¹, Jingyuan Liu¹, Xiaofeng Zhu¹, Zhichao Chu¹, Hao Le¹

¹China Institute of Atomic Energy, Beijing 102413, P R China

²FRIB, East Lansing, Michigan

Abstract

CIAE has proposed an innovative design for a 2 GeV, 6 MW isochronous FFA in 2019. This study aims to present the results of beam dynamics research, demonstrating the feasibility to accelerate the intense proton beam with the energy beyond 1 GeV limitation of isochronous cyclotrons. By introducing 1st - 3rd radial gradient of peak magnetic field to simulate the quadrupole to octupole component of the isochronous machine, three different lattice designs are obtained. Adjusting the radial gradient of the peak field allows an option to avoid or cross integer resonances. Various inherent and coupled resonances are investigated subsequently, with a focus on the destructive effects of the $\nu_r=3$ on the transverse phase space. Based on PIC method, we simulate the vortex motion caused by space charge in a large-scale alternating gradient field. Results indicated that the radial size of beam is ~ 10 mm, which is expected to be improved after considering the effects of neighboring bunches. Additionally, high-Q RF cavities and precession extraction further enlarge the turn separation to 30 mm, ensuring efficient beam extraction in the extraction region.

INTRODUCTION

High energy and high current proton accelerators are widely applied in frontier research fields such as nuclear physics and particle physics, national economic fields such as public health and advanced energy, and even national defence industry and national security [1][2]. Proton accelerator with an average beam power of 5-10 MW is the world's dream machine for more than 30 years [3][4]. Cyclotrons can provide continuous wave beam but are restrict by energy limitation ~ 1 GeV [5]. Beyond the traditional solutions for high intensity machines such as superconducting linac and rapid cycling synchrotron, CW FFA which is non-scaling and nonlinear was considered as an attractive proposal for several megawatts machine [6]. To utilize strong focusing optics and fixed frequency for CW acceleration, a 2 GeV/6 MW FFA concept design was proposed in 2019 [7]. In this machine, the F-D-F lattice design has been adopted to realize strong focusing. Each focusing and defocusing magnet has a third-order magnetic field gradient in the radial direction, which can achieve the effect of the dipole to octupole magnets, and thereby balance the isochronism and focusing. Based on this principle of adjusting gradient to provide strong focusing, higher-order nonlinear magnetic field components were added (such as quadrupole, hexapole, octupole, etc) to avoid important resonance crossings, resulting in a "radial local achromatic" effect. Three different lattice schemes (2019, 2020,

2022) are designed to achieve the goal of the isochronous acceleration for 2 GeV proton. The basic parameters of the three schemes are listed in Table 1. In this paper, beam dynamics of the 2 GeV/6 MW FFA is summarized for better comprehension of non-scaling and nonlinear FFA machines.

Table 1: Basic Parameters of 2 GeV CW FFA Machine

Parameters	Scheme 1	Scheme 2	Scheme 3
Extracted energy	2 GeV	2 GeV	2 GeV
Focusing magnet radius*	23.3~26.8 m	18.2~20.9 m	17.6~19.4 m
Defocusing magnet radius*	23.3~26.8 m	18.2~20.9 m	17.6~19.4 m
Focusing field	1.5~2.7 T	1.56~2.62 T	1.57~2.66 T
Defocusing field	1.0~2.4 T	1.77~2.51 T	1.15~2.31 T
Number of lattices	10	10	10
RF frequency	44.4 MHz	35.1 MHz	51.6 MHz
Cavity voltage (single cavity)	1.2 MeV	1.5 MeV	1.5 MeV
Harmonic number	26	16	22
Number of cavities	10	15	15
Turn separation for the extraction	~ 1.5 cm	~ 1.5 cm	~ 1.5 cm

* (From the machining center)

STATIC ORBITS ANALYSIS

Isochronism and Tune

It is well-known that static beam dynamics results are the basis for one to verify the feasibility of the lattice design. Therefore, the results of phase slip, tune diagram, and static region are introduced first.

The magnetic field of 2 GeV/6 MW machine (CYCIAE-2000) has the characteristics of high order gradient (up to 3rd), strong nonlinearity, etc. The physical design and beam dynamics study require higher tracking accuracy of the particle tracking program, especially near the edge field of focusing and defocusing magnets. Besides that, the beam dynamics simulation also needs higher magnetic field interpolation accuracy and more reasonable tracking algorithms which adaptive to wide-range twisty orbits of FFA. Some

STUDY OF THE KEY PHYSICS PROBLEMS IN 10mA-CLASS HIGH CURRENT CYCLOTRON

Tianjian Bian[†], Shizhong An, Fengping Guan, Luyu Ji, Sumin Wei
China Institute of Atomic Energy

Abstract

10MW-class ultra-high power cyclotron (UHPC) has great application prospects in cutting-edge sciences, neutron source, advanced energy and advanced material, etc. So far, Cyclotron with average beam power of 10 MW still have some bottleneck problems. Beam energy and current of a high-power cyclotron are typically less than 800MeV and 3mA. In this paper, bottleneck problems of UHPC are analysed, and then a preliminary design of UHPC-10MW is presented.

INTRODUCTION

GeV-class proton beam with an average power of several megawatts has many important applications in particle physics towards the intensity frontier, as well as in the advanced energy and material science. There are three different types of constructed accelerators for high power proton beam production: The cyclotron, linear accelerator and rapid-cycling synchrotron. The highest beam power of these accelerators currently is 1.4 MW. Reference [1] reported the energy efficiency of the three operational accelerators with the highest beam power in the world, which showed that the energy efficiency of the PSI cyclotron is about 2 times of the other types, as shown in Table 1. Weng made a judgement that the beam/grid efficiency should be better than 30%, otherwise the Accelerator Driven subcritical-reactor System(ADS) becomes nonsense 0. Studies have shown that the energy efficiency cyclotron is the highest which is expected to be 60%~65% in superconducting ring cyclotron 0. As cyclotron is a good technical route to develop proton machines with high beam power and high-power efficiency, it shows good prospect in advanced energy.

The beam power of UHPC-10MW aims at 10MW, it composes of two stages. The first stage is a 150MeV/amu injector and the second stage is a 1GeV/amu ring cyclotron. If UHPC-10MW is used to drive a spallation neutron source, the injector and the ring cyclotron can produce thermal neutron flux in the order of 10^{14} n/cm²/s and 10^{15} n/cm²/s, respectively. UHPC-10MW based spallation neutron source will have higher thermal neutron flux than high-flux reactor based neutron source. Even the 150MeV/amu injector can produce high thermal neutron flux which comparable to middle flux reactor neutron source. Figure 1 shows the history of thermal neutron

flux 0, and UHPC-10MW based spallation neutron sources are marked with stars.

Table 1: Efficiency of Different Types of High-Power Accelerators

Accelerator	Type	Energy (MeV)	Power (MW)	Efficiency
SNS	Linac	1000	1.3	8.6%
JPARC	synchrotron	3000	1.0	3%
SINQ	cyclotron	590	1.4	18%

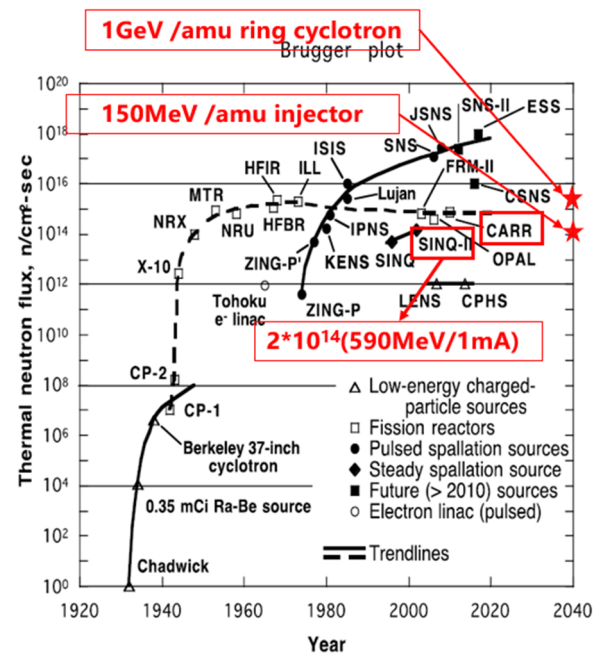


Figure 1: Thermal neutron flux history.

OVERALL DESIGN AND CONSIDERATION

Figure 2 shows the layout of UHPC-10MW. We choose a 1MeV/amu RFQ as the pre-injector, and a separate sector cyclotron accelerate the beam from RFQ to 150MeV/amu, finally the beam is injected to a 1GeV/amu ring cyclotron.

Superconducting linac is the mainstream of high-power accelerator, due to relative higher technical maturity. So far, no well-approved design of 10MW-class cyclotron is made due to some bottleneck problems. Radial tune is increasing linearly with beam energy in isochronous cyclotron, and thus the integer resonance crossing problem becomes an inevitable problem. Isochronous cyclotron is considered impossible to accelerate particles to a kinetic energy above its rest mass 0, typically 800MeV/amu.

* This work was supported by the National Natural Science Foundation of China (Grant No. 12105370) and the Scientific Research Program for Young Talent Elite Project of China National Nuclear Corporation (Grant No. FY212406000404).

[†] email address biantianjian@foxmail.com

TERAHERTZ-DRIVEN MeV ELECTRON BUNCH COMPRESSION AND STREAKING *

Y. Xu, Y. Song, J. Wang, C. Tsai, K. Fan[†], Z. Liu[‡], School of Electric and Electronic Engineering, Huazhong University of Science and Technology, Wuhan, China

Abstract

Electron bunches with ultra-short bunch length and ultra-high timing stability are crucial for various applications. To achieve these desired characteristics, there is a growing interest in employing Terahertz-driven techniques to manipulate and diagnose electron bunches. This paper presents a method capable of compressing and measuring electron bunch lengths. Theoretical and simulation results demonstrate that the bunch length of 54 fs is reduced to 4 fs by utilizing THz-driven resonant cavity compression, achieving a compression ratio of 13. Furthermore, we also verify the bunch compression using a terahertz-driven streak camera.

INTRODUCTION

Ultra-short and precisely timed electron bunches are essential for applications such as ultrafast electron diffraction (UED) and free-electron lasers (FELs) [1-3]. In UED, the temporal resolution relies on the quality of the electron bunch used as a probe. Both the bunch length and the timing jitter relative to the laser can impact the overall system resolution. RF deflecting cavities are commonly employed to compress the bunch length while maintaining low emittance [4-5]. However, the phase jitter of the RF resonant field introduces energy instability to the electron bunch, resulting in a time-of-arrival (TOA) jitter typically ranging from tens to hundreds of femtoseconds. THz-driven bunch manipulation enables the generation of electron bunches with femtosecond-scale lengths and high-timing stability.

This all-optical method ensures inherent synchronization between the THz field and the electron bunch, enabling precise manipulation without inducing time jitter [6]. Various demonstrations of THz-driven techniques have been reported. For example, butterfly-shaped resonators compress and diagnose keV-level electron bunches [7], and parallel-plate waveguide structures compress MeV-level electron bunches [8]. The segmented terahertz electron accelerator and manipulator (STEAM) structure offers a multifunctional design for compression and measurement [9]. These studies highlight the potential of strong-field THz techniques for manipulating and diagnosing electron bunches.

This paper presents a method illustrated in Fig. 1 to compress and diagnose electron bunches using THz-driven resonators. A buncher generates a longitudinally polarized field for compressing the electron bunch length, while a slit downstream serves as a THz-driven streak camera to measure the bunch length. Despite the space charge effect

causing continuous expansion in both longitudinal and transverse directions, passing the electron bunch through the THz electric field at the zero-crossing phase achieves opposite momenta for the head and tail electrons, resulting in the minimum bunch length at the sample position. At this position, a transversely polarized THz field generated by the slit converts the electron bunch's longitudinal temporal information into a transverse bunch distribution. Analyzing the measurements from the detector allows us to infer the bunch length and time of arrival. The effectiveness has been verified through theoretical analysis and numerical simulations, demonstrating its capability to compress and evaluate MeV-level electron bunches.

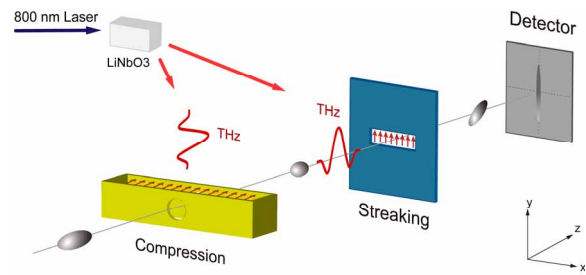


Figure 1: Schematic of the compression and streaking system.

THz-DRIVEN ELECTRON BUNCH COMPRESSION

Figure 2 illustrates the THz buncher structure along with its equivalent LC circuit model, which can be simplified as a resonator. The driving THz driving pulse, polarized along the z-axis, enters the buncher from the top. As a result of resonance, an enhanced THz field is generated in the gap, with the amplitude and frequency dependent on both the driving THz pulse and the buncher geometric parameters. The THz electric field mainly concentrates near the channel through which the electron beam passes and has a uniform amplitude, as shown in Fig. 2 (b).

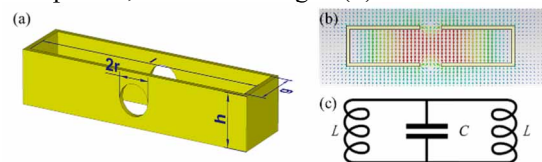


Figure 2: (a) The structure of the THz buncher. (b) The electric field distribution in buncher. (c) The equivalent LC circuit of the buncher.

Due to the structural symmetry, the gap exhibits a strong electric field while having an almost negligible magnetic field. These characteristics make the buncher well-suited for beam compression. When an electron beam passes

* Work supported by NSFC 12235005 and the State Grid Corporation of China Technology Project 5400-202199556A-0-5-ZN

[†]kjfan@hust.edu.cn, [‡]zzliu@hust.edu.cn

STUDY ON A POLARIZATION CONTROLLABLE UNDULATOR FOR HIGH-GAIN FREE ELECTRON LASERS *

Ruixuan Huang[†], Qika Jia[‡],

University of Science and Technology of China, Hefei, 230026 China

Lijun Chen,

China Academy of Engineering Physics, Mianyang, 621900 China

Abstract

SASE FEL can generate intense and coherent linearly-polarized X-ray when high energy electron beams travelling through a long planar undulator. It is also of great importance and interest to control the polarization of FEL. One possible solution is utilizing a customized undulator to adjust the magnetic field direction. By tuning the displacement of the magnetic block arrangement, variation of polarization could be achieved. In this paper we study on a polarization controllable undulator to realize the variable polarized magnetic field. Different shapes and design considerations of the magnetic block configuration will be introduced. The value of peak field and the region of good field will be analysed and discussed.

INTRODUCTION

The X-ray free electron laser (FEL) have the ability to explore the ultra-small and ultra-fast regime. Self-amplified spontaneous emission (SASE) is intense and coherent radiation via an extremely high gain process. SASE FEL usually produces linearly polarized radiation based on planar undulators. The light source polarization is one of the key characteristics of the radiation. Furthermore, arbitrarily polarization control has great application requirement, such as in developing powerful probing spectroscopies [1] and performing circular dichroism experiments [2]. A helical undulator could be used to achieve circular polarization, while challenging to change the polarization between two diametrically opposed helices. Another method to obtain control of polarization is to use a dedicated planar undulator. By tuning the relative displacement between upper and lower magnet array, the phase of the electromagnetic field is shifted and the field strength is adjusted, turning out the polarization change. In this manuscript, we will give the study of different shapes and design considerations of the magnetic block configuration.

MAGNETIC STRUCTURE

We have studied a novel variable elliptical polarization undulator with different structure arrangement considered. In the original design, the pure permanent magnetic blocks are periodically arranged with four upper and lower blocks. In each period, two opposite horizontal magnetization of

magnets and two opposite longitudinal magnetization of magnets are placed at intervals. The displacement of upper and lower magnet arrays can be mechanically shifted. As a result, a horizontal polarization, a vertical polarization and an elliptical (or circular) polarization can be realized separately. Several magnetic block shapes are considered as shown in Fig. 1.

The magnetic design is performed via the Radia package [3]. In one design specification of the original structure, the simulation results for different polarization modes of the transverse magnetic field distribution on the longitudinal axis are shown in Fig. 2. Undulator parameters of the original block and displacement shift requirement on polarization change are listed in Table 1. The peak field of the periodic distribution can reach above 0.4 T for linear polarizations, and above 0.3 T for circular polarization. Although there is field deformation at ends of the undulator, it can be improved by optimization of the edge blocks. However, the uniform region very small for this original structure. Some techniques have been suggested to improve the transverse field homogeneity [4,5]. We study on three design considerations.

Table 1: Main Parameters of the Original Block Design

Parameter	Specification
Period	100 mm
Number of periods	10
Gap(fixed)	20 mm
Magnet block size(width*height)	60*60 mm
Vertical peak field	0.42 T
Horizontal peak field	0.44 T
Peak field at circular polarization	0.33 T
Shift of vertical polarization	0 mm
Shift of horizontal polarization	50 mm
Shift of circular polarization	35.6 mm

Side-block Arrangement

In the side-block arrangement, magnet blocks of vertical magnetization are added at both width end of the horizontal magnetization blocks to compensate the region of good field. By proper optimize the geometrical parameters, the uniform field region is increased from less than 0.1 mm to 1.0 mm in horizontal and 1.8 mm in vertical, under field homogeneity $\Delta B/B \leq 0.5\%$.

We fix the size of the main magnets and the height of the side blocks, then compare the peak field and the uniform

* Work supported by the National Natural Science Foundation of China (Grant Number 12175224, 11805200).

[†] rxhuang@ustc.edu.cn

[‡] jiaqk@ustc.edu.cn

LOWEST LONGITUDINAL AND TRANSVERSE RESISTIVE-WALL WAKE AND IMPEDANCE FOR NONULTRA-RELATIVISTIC BEAMS*

J. Tang[†]

Tsinghua University in Beijing (TUB) Accelerator Laboratory Department of Engineering Physics

Abstract

With the development of the steady state micro bunching (SSMB) storage ring, its parameters reveal that the ultra-relativistic assumption which is widely used is not valid for the electron beam bunch train, which has length in the 100nm range, spacing of 1μm and energy in hundreds MeV range. The strength of the interaction between such bunches and the potential instability may need careful evaluation. At the same time, the effect of the space charge inside a single bunch due to space charge effect also needs to be considered. In this article, we reorganized the lowest-order longitudinal wakefield under non-ultra relativistic conditions, and modified the inconsistent part in the theoretical derivation in some essays of the lowest-order transverse wakefield. We present the modified theoretical results and analysis. The action area are then divided into three parts. It lays foundation in future research.

INTRODUCTION

Based on published literature, we have reorganized the lowest-order longitudinal wakefield under nonultra-relativistic conditions which is the monopole longitudinal wakefield, and we have modified the inconsistent part in the theoretical derivation of the lowest-order transverse wakefield which is the dipole transverse wakefield in existing literature. We present the modified theoretical results and analysis. The calculation results are evaluated, and the action area of the non-ultra relativistic wakefield is divided into a short-range dominated by the source charge space force, a middle section dominated by the mirror space charge force, and a long-range resistive wall that can be estimated using classical ultra-relativistic assumption. This lays the foundation and clarifies the ideas for subsequent beam dynamics analysis.

LONGITUDINAL WAKEFIELD

Previous Result

The classical Longitudinal Wakefield for multipole has an analytical expression [1]

$$W_m(z) = -\frac{c}{\pi b^{2m+1} (1 + \delta_{m0})} \sqrt{\frac{Z_0}{\pi \sigma_c}} \frac{L}{|z|^{\frac{1}{2}}} \quad (1)$$

$$W'_m(z) = -\frac{c}{2\pi b^{2m+1} (1 + \delta_{m0})} \sqrt{\frac{Z_0}{\pi \sigma_c}} \frac{L}{|z|^{\frac{3}{2}}} \quad (2)$$

where b is the radius of the pipe, σ_c is the conductivity of the surrounding medal. This result is obtained by ultra-relativistic limit $\gamma \rightarrow +\infty$, e.g. the speed of the electron is the speed of light c . Meanwhile, the effective region of the longitudinal coordinate is

$$\chi^{\frac{1}{3}} b \ll |z| \ll \chi^{-\frac{1}{3}} \frac{c}{b}, \quad z < 0 \quad (3)$$

where $\chi = \frac{1}{\mu \sigma_c b c}$. For Aluminum pipe whose radius is in several centimeters range, the effective region will be $1.95 \times 10^{-5} m \ll z \ll 1.54 \times 10^{13} m$.

In order to calculate short range wakefield, in SLAC-PUV-95-7074 [2] there is a formula for longitudinal Electric Field in the time-space domain

$$E_z^m(z) = -16\gamma \left(\frac{1}{3} e^{-\gamma \frac{z}{s_0}} \cos \frac{\sqrt{3}\gamma \frac{z}{s_0}}{s_0} - \frac{\sqrt{2}\gamma}{\pi} \int_0^\infty \frac{x^2 e^{-x^2 \frac{z}{s_0}}}{x^6 + 8\gamma^2} \right) \quad (4)$$

where

$$s_0 = b^{\frac{1}{2}} \left(\frac{c}{2\pi\sigma} \right)^{\frac{1}{3}} \quad (5)$$

this equation is valid for all $z \leq 0$.

SSMB Case Monopole Wake Benchmark

For the SSMB Parameters showed at Table 1 reveal that the space charge effect estimate by $\frac{2b}{\gamma}$ would be about 30.6 μm. Such an effective length would be much larger than the spacing between bunch to bunch. So, it would be better that we consider if it is appropriate to view space charge electromagnetic field as a round plate.

Table 1: SSMB Bunch Train Parameters

Parameter	Value	Purpose
Length	10 nm	Longitudinal Coherent
Transverse size	10–100 μm	
Spacing	1 μm	High Average Power
Energy	250 MeV	$\gamma \approx 490.2$

There is such a monopole result derived for nonultra-relativistic beam [3, 4] by solving the Maxwell equation by Fourier Transformation, the longitudinal impedance is showed as Eq. (7). And when we get the expression of the impedance, we can obtain the Longitudinal Wake Field through Inverse Fourier Transformation.

$$W'_0(z, r) = \frac{1}{2\pi v} \int_{-\infty}^{\infty} Z_{\parallel}(\omega, r) e^{\frac{i\omega z}{v}} d\omega \quad (6)$$

* Work supported by Tsinghua University Accelerator Laboratory

[†] tjz21@mails.tsinghua.edu.cn

DESIGN OF BEAM DYNAMICS FOR A HIGH-POWER DC PROTON ACCELERATOR AT THE MeV LEVEL*

Zi-Feng He[#], Minghua Zhao, Shanghai Institute of Applied Physics, Chinese Academy of Sciences,
Shanghai 201800, China

Weishi Wan, Shanghai University of Science and Technology, Shanghai 201210, China

Abstract

This paper aims to design the beam dynamics of a MeV-level high-power DC proton accelerator for use in high-voltage accelerators. The high-power proton accelerator has essential applications such as ion implantation equipment, neutron therapy equipment, and accelerator-based neutron source equipment. With the increasing use of high-voltage generators due to their stable and reliable operation, these accelerators have gained significant popularity in the field. The paper discusses the design considerations of the accelerator equipment, including the functions and requirements of the acceleration tube, electric field distribution, and voltage holding issues. Additionally, the paper focuses on the design aspects of beam optics, encompassing topics such as electric field distribution, beam focusing, beam transmission, divergence, and the impact of space charge effects on beam quality. Calculations and optimizations are performed based on the parameters and requirements specific to high-voltage accelerators. Finally, the paper presents and analyzes the results of the accelerator tube and beam optics design.

INTRODUCTION

MeV-level proton accelerators, as powerful and versatile particle acceleration devices, play a significant role in various industries, scientific research, and medical applications. In the industrial sector, MeV-level proton accelerators are widely utilized in material processing and surface treatment techniques, enabling high-energy material modification and ion implantation processes. In the field of scientific research, MeV-level proton accelerators provide robust tools for nuclear physics and particle physics investigations. In the medical domain, MeV-level high-power DC proton accelerators generate high-power proton beams that produce neutrons through target interactions. These neutrons are utilized in Boron Neutron Capture Therapy (BNCT) for targeted tumor radiation treatment. For MeV-level high-power DC proton accelerators operating with a single-ended electrostatic acceleration scheme, beam optics design becomes particularly crucial.

DESIGN ISSUES OF ACCELERATOR TUBES

Beam Parameters of the Incident Ion Beam in the Accelerator Tube

Based on the output characteristics of the high-current DC microwave ion source [1-3], the beam parameters of the incident ion beam in the accelerator tube can be set as shown in the Table 1.

Table 1: Parameters of the Incident Beam at the Entrance of the Accelerator Tube

Parameters	Value
Emittance ϵ	0.5π mm mrad
α	0.2
β	0.4 mm/mrad
Spot diameter	4 mm

The Space Charge Effect of the Ion Beam

As the current passing through the accelerator tube increases, the effect of space charge becomes more significant, leading to an increase in the radius of the ion beam and a deterioration in the focusing properties of the accelerator tube system. Consequently, more current is lost on the electrodes, resulting in a sharp increase in the load on the accelerator tube due to secondary electrons. The simulation results for proton beams with beam currents of 0.1 mA, 1 mA, and 15 mA, initial energy of 40 keV, and a 1 cm beam spot radius drifting in an infinite space are shown in Figure 1.

The radial potential distribution of the ion beam is a crucial aspect of the accelerator's beam dynamics, as shown in Figure 2. It describes the variation of electric potential across the radial dimension of the ion beam.

Considering the ion beam to be infinitely long and axially symmetric, the potential distribution function generated by space charge is determined by the following equation.

$$U(r) = \begin{cases} \frac{\rho r_b^2}{4\epsilon_0} \left[1 + 2 \ln \left(\frac{R}{r_b} \right) - \left(\frac{r}{r_b} \right)^2 \right], & 0 \leq r \leq r_b \\ \frac{\rho r_b^2}{4\epsilon_0} \ln \left(\frac{R}{r_b} \right), & r_b \leq r \leq R \end{cases} \quad (1)$$

* Work supported by Major Development Project of the Shanghai Institute of Applied Physics, CAS [Y951011031].
hezifeng@sinap.ac.cn

APPROXIMATION OF SPACE CHARGE EFFECT IN THE PRESENCE OF LONGITUDINAL MAGNETIC FIELDS

H. Y. Li[†], J. R. Shi, H. Zha^{*}, W. H. Gu, Q. Gao, H. B. Chen, Tsinghua University, Beijing, China

Abstract

The space charge effect plays a significant role in the evolution of phase space during beam transport. Applying an external longitudinal magnetic field has been shown to effectively reduce beam expansion through the mechanism of beam rotation. In this article, we present a fast approximation algorithm for estimating the impact of an external magnetic field on beam expansion. The algorithm enables efficient computations and provides insights into controlling the phase space dynamics of the beam in the presence of longitudinal magnetic fields.

INTRODUCTION

In particle accelerators, space charge forces have a significant impact on the transmission process, causing the beam to expand in both the transversal and longitudinal dimensions. This expansion leads to an increase in emittance, the formation of beam halo, and even beam loss [1]. Notably, the space charge force is proportional to $1/\gamma^2$, where γ represents the Lorentz factor [2]. Therefore, the influence of the space charge force becomes more pronounced for low-energy high-intensity beams. As the transmission distance increases, the impact of the space charge force on high-energy beams gradually becomes significant. In the simplest scenario, using an infinitely long uniform beam model, the expression for the space charge force can be given as follows:

$$F_r = \frac{qI r}{2\pi\epsilon_0\beta c a^2 \gamma^2} \quad (1)$$

As shown in Figure 1, a is the radius of the beam.

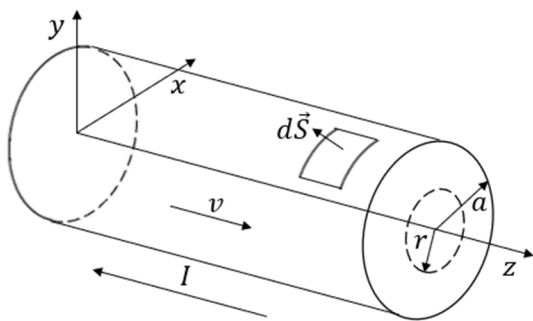


Figure 1: The infinitely long uniform beam model.

When a longitudinal magnetic field B is applied, it can help alleviate the space charge effect. As macroparticles

experience space charge forces and gain radial velocity, the Lorentz force causes the beam to rotate in the angular direction. This rotation dissipates some of the total energy derived from the electromagnetic potential. Consequently, this process can effectively slow down the radial expansion of the beam.

Furthermore, the angular rotation of particles gives rise to an induced longitudinal magnetic field B_1 , which acts to weaken the original magnetic field B . However, through simulation, it has been observed that B_1 is significantly smaller than B . Consequently, in the subsequent discussion, we will neglect the influence of B_1 . Additionally, we assume that the transverse velocity is much smaller than the longitudinal velocity, which is close to the speed of light. In the Cartesian coordinate system, with the longitudinal direction defined as the z -axis, the equation of motion for the macroparticles can be expressed as follows:

$$\ddot{x} = A_1 x - A_2 \dot{y}; \quad \ddot{y} = A_1 y + A_2 \dot{x} \quad (2)$$

Wherein $A_1 = qI/\gamma^3 m_0 2\pi\epsilon_0\beta c a^2$; $A_2 = qB/\gamma m_0$. m_0 is the static mass of an electron. By utilizing the fourth-order Runge-Kutta method, we can update the position of a macroparticle based on an appropriate time step. This numerical technique allows us to accurately calculate the particle's trajectory and track its motion throughout the simulation.

From Eq. (1) and Eq. (2), we observe that in a uniform electron beam, the accelerations and velocities of particles are both proportional to their radial positions. As a result, after expansion, the ratio of radial coordinates for different particles remains constant, indicating that the beam remains uniform. In order to simplify the computation, a fast approximation algorithm can be employed, where only the motion of the outermost particle is calculated. This approximation allows for a more efficient calculation process while still capturing the overall behaviour of the beam.

PROGRESS

Verification with Astra

We have developed a fast approximation algorithm utilizing Eq. (1) and Eq. (2). In order to validate the accuracy of this approximation algorithm, we can compare its results with those obtained from Astra, a space charge tracking algorithm developed by DESY [3]. For this comparison, we can utilize the single-bunch model. If the length of the beam remains relatively constant after transport, its equivalent current can be considered constant as well. Under such circumstances, Astra's finite-cylinder model is equivalent to the infinitely long beam model. By comparing the results of our approximation algorithm with Astra's

[†] li-hy22@mails.tsinghua.edu.cn
^{*} zha_hao@tsinghua.edu.cn

IMPACT OF NEG COATING THICKNESS AND RESISTIVITY ON BEAM COUPLING IMPEDANCE

Tianlong He*, Weiwei Li, Zhenghe Bai, Hongliang Xu[†]
National Synchrotron Radiation Laboratory, USTC, Hefei 230029, China

Abstract

In diffraction-limited storage rings, non-evaporable getter (NEG) coatings are generally used to assure the ultrahigh vacuum, which, however, also increase the beam coupling impedance that can affect beam dynamics. Ignoring the influence of coating roughness, the impact of NEG coatings on the impedance mainly depends on the coating thickness and resistivity. In this paper, we investigate the impedance characteristics of a round CuCrZr vacuum chamber coated by NEG with different thickness and resistivity.

INTRODUCTION

For diffraction-limited storage rings (DLSRs) designed based on multi-bend achromat lattice, its vacuum chamber size is generally limited by the requirements for high gradient multipole magnets and high performance insertion devices. Small vacuum chamber is not conducive to maintaining the ultra-high vacuum environment for beam circulating in the ring. To assure the ultra-high vacuum, it is necessary to make a layer of NEG coating on the inner surface of vacuum chamber to improve the pumping speed [1]. However, NEG coating will increase significantly the resistive wall (RW) impedance especially in the high frequency region, resulting in a reduction in the threshold of single bunch instabilities, e.g., microwave instability and transverse mode coupling instability [2].

For vacuum chambers with NEG coating, the IW2D (ImpedanceWake2D) code is most widely used to calculate the RW impedance [3, 4]. For ease of impedance calculation in the windows operating system, we referred to the core source code of IW2D and wrote a Mathematica script to substitute for IW2D. After debugging, both results were basically consistent. Therefore, all impedance calculations in this paper were performed using this Mathematica script.

To calculate the RW impedance, in addition to the parameters of vacuum chamber, generally, two key parameters of NEG coating are required to set: thickness and resistivity. For DLSRs, the coating thickness is usually around 1 μm [1], and the coating resistivity, depending on the coating method, often varies in the range of $1.25 \times 10^{-6} \sim 7.1 \times 10^{-5} \Omega \cdot \text{m}$ [5]. It naturally leads to the question: what is the best choice of the thickness and resistivity of NEG coating for mitigating its influence on the RW impedance? To answer this question, it is better to sweep the two parameters and evaluate the impedance accordingly. Once obtained the impedance data, we can further calculate the longitudinal loss factor

and transverse kick factor to preliminarily assess the impact of NEG coating.

THEORY AND METHOD

Impedance Calculation

As mentioned earlier, we used a Mathematica script (equivalent to IW2D) for NEG coating parameter sweeping calculation. The resistivity and thickness of NEG coating are swept in the range of $1 \times 10^{-7} \sim 1 \times 10^{-4} \Omega \cdot \text{m}$ and $0.1 \sim 2 \mu\text{m}$, respectively. The round vacuum chamber is assumed to have a radius of 11 mm and material of CuCrZr with resistivity of $\rho = 2.18 \times 10^{-8} \Omega \cdot \text{m}$.

Loss Factor and Kick Factor

For a Gaussian bunch, the loss factor and the kick factor are respectively given by :

$$K_{loss} = \frac{\omega_0}{2\pi} \sum_{p=-\infty}^{\infty} \text{Re}[Z_{\parallel}(p\omega_0)] \exp[-(p\omega_0\sigma_t)^2], \quad (1)$$

and

$$K_{\perp} = -\frac{\omega_0}{2\pi} \sum_{p=-\infty}^{\infty} \text{Im}[Z_{\perp}(p\omega_0)] \exp[-(p\omega_0\sigma_t)^2], \quad (2)$$

where σ_t is the rms bunch length, ω_0 is the revolution angular frequency, p is an integer, $\text{Re}[Z_{\parallel}]$ is the real part of the longitudinal RW impedance and $\text{Im}[Z_{\perp}]$ is the imaginary part of the transverse RW impedance.

IMPACT OF NEG COATING

Impact of NEG Coating Resistivity on Impedance

Figures 1 and 2 show the longitudinal and transverse RW impedances of per-unit-length vacuum chamber with a 1 μm NEG coating, respectively. It is obvious that the NEG coating mainly affects the impedance behaviour in the frequency region of higher than 10 GHz. It should be noted, in this frequency region, that the impedance behaves like a resonator, and the resonant peak of the real part gets higher and the corresponding bandwidth gets narrower with the increase of resistivity. For the cases of resistivity in $5 \times 10^{-6} \sim 1 \times 10^{-4} \Omega \cdot \text{m}$, the difference among them is small. It indicates that, with the resistivity in this range, the impact of NEG coating on the longitudinal and transverse impedance has a weak dependence on resistivity. For the case of resistivity in $1 \times 10^{-7} \sim 5 \times 10^{-6} \Omega \cdot \text{m}$, the imaginary part significantly decreases with a decrease in resistivity, while the real part exhibits complexity as shown in Figs. 1 and 2(top) where different curves cross each other in $10^{10} \sim 10^{13}$ Hz.

* htlong@ustc.edu.cn

[†] hlxu@ustc.edu.cn

DEVELOPMENT OF A VLASOV SOLVER FOR ARBITRARY SUB-OPTIMAL LENGTHENING CONDITIONS IN DOUBLE-RF SYSTEM

Jingye Xu¹, Institute of High Energy Physics (IHEP), Chinese Academy of Sciences, Beijing, China*

Chuntao Lin, Institute of Advanced Science Facilities (IASF), Shenzhen, China

Na Wang¹, Haisheng Xu¹, Yuan Zhang¹, Institute of High Energy Physics (IHEP),
Chinese Academy of Sciences, Beijing, China

¹ also at University of Chinese Academy of Sciences (UCAS), Beijing, China

Abstract

Solving Vlasov equation is a classic method for analyzing collective beam instabilities. Considering longitudinal impedance and the nonlinear longitudinal potential well, we developed a new Vlasov solver which can be used to study the transverse mode-coupling instability under the arbitrary sub-optimal lengthening and the optimal lengthening conditions in a double-RF system. Several different techniques to deal with the radial direction of longitudinal phase space have been tested. Numerical discretization method is selected in this paper. The development of the solver is presented in details here. Benchmarks and crosscheck of the solver have been made and presented as well.

INTRODUCTION

Most (semi-)analytical Vlasov solvers are based on a single RF cavity or do not contain synchrotron tune spread [1,2]. In 2014, A. Burov proposed the NHTVS (Nested Head-Tail Vlasov Solver), which can contain small synchrotron tune spread but it is based on Gaussian bunches [3]. In 2018, Venturini proposed radial discretization which contains large synchrotron tune spread and flat-top distribution, it is only applicable for optimal lengthening. [4]. They may result in significant errors under conditions where the longitudinal distribution is completely different from Gaussian or the synchrotron tune spread cannot be ignored. There is currently no general Vlasov solver for sub-optimal lengthening conditions.

In this paper, we proposed a method to deal with arbitrary sub-optimal lengthening bunch by discretization of Vlasov equation. It is a general method to dominate Gaussian, sub-optimal and optimal lengthening bunches.

At first, we will derivate Vlasov equation similar to Ref. [5]. Then we choosed two typical cases and compared our method with Chuntao Lin's transfer matrix method [6]. The specific sampling process will be described in this section.

* xujingye@ihep.ac.cn

FORMULA DERIVATION

The single-particle equations of motion are:

$$\begin{cases} \dot{y}(s) = p_y \\ \dot{p}_y(s) = - \left(\frac{\omega_\beta}{c} \right)^2 y + \frac{1}{E} F_y(z, s) \\ \dot{z}(s) = - \eta_p \delta \\ \dot{\delta}(s) = \frac{eV_1}{EC} \mathcal{V}'(z) \end{cases} \quad (1)$$

Here F_y is transverse wake force, E is particle energy, ω_β is betatron frequency, η_p is slippage factor, C is circumference of the storage ring, and $V_1 \mathcal{V}'(z)$ is the voltage of double RF system, where

$$\begin{aligned} \mathcal{V}'(z) = & \sin \left(\phi_s - \frac{2h_1\pi}{C} z \right) - \sin \phi_s \\ & + r \sin \left[\phi_{2s} - \frac{2h_1 h\pi}{C} z \right] - r \sin \phi_{2s}. \end{aligned} \quad (2)$$

We use action-angle variables J, ϕ in the longitudinal phase space and polar coordinates q, θ in the transverse. So the perturbation formalism of density distribution $\psi(J, \phi, q, \theta; s)$ can be written as

$$\psi = f_0(q)g_0(J) + f_1(q, \theta)g_1(J, \phi)e^{-i\Omega s/c}.$$

Substitute ψ , Eqs. (6.168) and (6.173) in Ref. [5] into the Vlasov equation,

$$\begin{aligned} i(\Omega - \omega_\beta)g_1 = & \frac{ce^2}{2E\omega_\beta T_0^2} g_0 \sum_p \tilde{\rho}_1(\omega') Z_1^\perp(\omega') e^{i\omega' z/c} \\ & + B(J, \phi) \left[\frac{\partial g_1}{\partial J} - \frac{1}{D} \frac{f_0'}{f_0} \frac{\partial g_0}{\partial J} e^{i\Omega s/c - i\theta} \right] + C(J, \phi) \frac{\partial g_1}{\partial \phi}, \end{aligned} \quad (3)$$

here

$$\begin{aligned} B(J, \phi) = & \dot{\delta}(z) \frac{\partial J}{\partial \delta} \Big|_z + \dot{z}(t) \frac{\partial J}{\partial z} \Big|_s = \frac{d\vec{r}(t)}{dt} \cdot \nabla J = \frac{dJ}{dt} = 0, \\ C(J, \phi) = & \dot{\delta}(z) \frac{\partial \phi}{\partial \delta} \Big|_z + \dot{z}(t) \frac{\partial \phi}{\partial z} \Big|_s = \frac{d\vec{r}(t)}{dt} \cdot \nabla \phi = \omega_s(J). \end{aligned} \quad (4)$$

Here \vec{r} is the vector from the original point to the particle coordinate (z, δ) in the longitudinal phase space. By the same manipulation of Fourier expansion of g_1 in Ref. [5],

MATCHING SECTION DESIGN AT THE MeV ULTRAFAST ELECTRON BEAM EXPERIMENTAL FACILITY

H. Qi, C.-Y. Tsai, J. Wang, Z. Z. Liu[†], K. J. Fan[†]
Huazhong University of Science and Technology, Wuhan, China

Abstract

This paper introduces the design and optimization of the matching section beamline for the ultrafast electron research platform at Huazhong University of Science and Technology (HUST). The matching section serves as a connection between the main beamline and the beam physics research beamline, aiming to achieve efficient and precise control over the electron beam trajectory and parameters. To evaluate its performance, particle tracking simulations using GPT software were conducted. When the beam is set at 3 MeV and 1 pC charge, the matching section is capable of compressing the bunch length to approximately 50 fs. This level of compression is crucial for ultrafast electron research applications, as it enables the study of phenomena that occur on extremely short time scales, demonstrating its effectiveness in achieving precise beam control and compression.

INTRODUCTION

The ever increasing demand for high-power and wide-band THz radiation has led to its growth in various research fields such as communication [1], biological imaging [2], and plasma diagnostics [3]. To address this demand, we are currently developing a second beamline at HUST that will focus on beam physics research, specifically investigating terahertz radiation and beam Space-Charge (SC) effects.

Figure 1 illustrates the layout of the MeV ultrafast electron beam experimental facility at Huazhong University of Science and Technology (HUST), featuring two beam lines. The primary beamline is dedicated to achieving sub-100 fs time resolution in a MeV ultrafast electron diffraction (UED) setup [4]. The second beamline is connected to the downstream experimental facility through a matching section [5,6], which serves multiple purposes: bending the electron beam and further compressing the bunch.

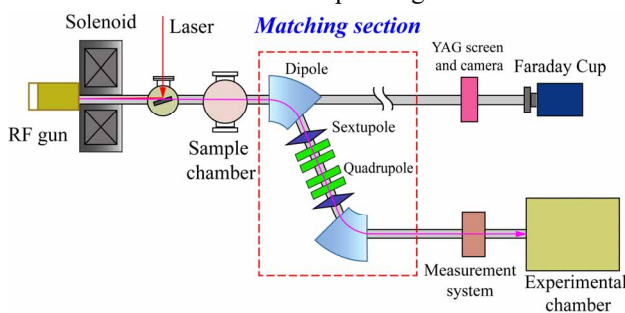


Figure 1: Schematic of the proposed MeV HUST facility.

* Work supported by the National Natural Science Foundation of China (NSFC 12235005 and 12275094), and National key research and development program of China (2022YFA1602202).

[†] kjfan@hust.edu.cn; [†] zzliu@hust.edu.cn

Typically, a matching section consists of two dipoles along with quadrupoles and sextupoles that help mitigate dispersion. In the matching section, an electron beam with energy chirp undergoes phase rotation. Through careful design, a positive energy chirp is transformed into a negative chirp, leading to beam compression and ultimately reaching a beam waist downstream. This optimization ensures efficient and compact electron beam propagation.

BEAM OPTICS DESIGN

During the initial design phase of the matching section, it is typically adequate to consider the first-order beam transport matrix. This matrix, denoted as R , describes the transformation of beam parameters from the entrance to the exit of the matching section.

In the matching section, R is composed of the transport matrices of the dipole, quadrupole, and drift elements [7-9]. The linearized form of R can be expressed as follows:

$$R = \begin{bmatrix} R_{11} & R_{12} & 0 & 0 & 0 & R_{16} \\ R_{21} & R_{22} & 0 & 0 & 0 & R_{26} \\ 0 & 0 & R_{33} & R_{34} & 0 & 0 \\ 0 & 0 & R_{43} & R_{44} & 0 & 0 \\ R_{51} & R_{52} & 0 & 0 & 1 & R_{56} \\ 0 & 0 & 0 & 0 & 0 & 1 \end{bmatrix}. \quad (1)$$

The explicit expression of the transport matrix R for the matching section can be obtained by straightforwardly multiplying the transport matrices of each individual element.

Since the matching section serves as a bunch compressor for the second beamline, it is essential to ensure that the energy chirp becomes negative at the exit in order to generate the longitudinal beam waist downstream. This requirement imposes a condition on the transport matrix R of the matching section, specifically that the matrix element R_{56} must be less than zero. Furthermore, the dipole magnets in the matching section introduce a dispersion term that cannot be ignored, which can cause a significant transverse position offset and result in beam loss. To mitigate this issue, dispersion matching becomes necessary, which involves setting the matrix elements R_{16} and R_{26} to zero at the exit of the matching section, effectively eliminating the leakage of dispersion.

The matching section implemented at the HUST experimental facility is designed to be symmetric, and its specific layout is illustrated in Fig. 2. The dipole magnet in this section has a bending angle (θ) of 60 degrees and an effective radius (ρ) of 0.26 m. Between the two dipole magnets, four

ANALYSIS OF THE FLUCTUATION OF RESONANCE DRIVING TERMS FOR NONLINEAR LATTICE OPTIMIZATION

Bingfeng Wei, Jiajie Tan, Zhenghe Bai*, Guangyao Feng[†]
National Synchrotron Radiation Laboratory, USTC, Hefei, China

Abstract

Minimizing resonance driving terms (RDTs) of nonlinear magnets is a traditional approach to enlarge the dynamic aperture (DA) of a storage ring. The local cancellation of nonlinear dynamics, which is adopted by some diffraction-limited storage rings, is more effective than the global cancellation. The former has smaller fluctuation of RDTs along the ring. In this paper, the correlation between two kinds of RDT fluctuations is found. The physical analysis shows that minimizing the RDT fluctuations is beneficial for controlling the crossing terms and thus enlarging the DA. This physical analysis is supported by the statistical analysis of nonlinear solutions of a double-bend achromat lattice.

INTRODUCTION

The widely-used analytical approach for the nonlinear optimization of storage rings is to minimize resonance driving terms (RDTs) of nonlinear magnets. In this approach, the Hamiltonian for particle motion is split into linear and nonlinear parts, and the nonlinear parts is expanded as the resonance basis, i.e. RDTs [1]. Minimizing the RDTs can control the corresponding resonance and thus enlarge the dynamic aperture (DA). The local nonlinear cancellation, which is used in the lattice design of some diffraction-limited storage rings, is more effective than the global cancellation [2]. And the former has smaller fluctuation of RDTs along the ring. There are two ways to calculate the longitudinal fluctuation of RDTs. One is to calculate the accumulated RDTs with a fixed starting position, and the build-up and cancellation of RDTs are shown in this way. We call it the RDT build-up fluctuation. We have shown that minimizing the RDT build-up fluctuations is more effective than minimizing the commonly used one-turn RDTs in enlarging the DA [3]. The other is to calculate the one-turn map (or one-period map) with varying longitudinal starting position [4]. In this paper, we will study the correlation between these two kinds of RDT fluctuations. And then we will analyze the effects of minimizing the RDT fluctuations.

RELATION BETWEEN TWO KINDS OF RDT FLUCTUATIONS

For a storage ring lattice with N sextupoles, the one-period map observed at s_0 is

$$\mathcal{M}(s_0) = \mathcal{A}_{s_0}^{-1} e^{i\mathcal{H}} \mathcal{R} \mathcal{A}_{s_0}, \quad (1)$$

where \mathcal{A}_{s_0} is a normalizing map, \mathcal{R} is a rotation, and $e^{i\mathcal{H}}$ is the nonlinear Lie map. For the on-momentum particles, the n -th order generator of $e^{i\mathcal{H}}$ can be expanded as:

$$h_n = \sum_{j+k+l+m=n} h_{jklm} h_x^{+j} h_x^{-k} h_y^{+l} h_y^{-m}, \quad (2)$$

where $h_x^\pm \equiv \sqrt{2J_x} e^{\pm i\phi_x}$, $h_y^\pm \equiv \sqrt{2J_y} e^{\pm i\phi_y}$, with (J, ϕ) being action-angle variables, and h_{jklm} is the driving terms. For any thin sextupole a , its normalized Hamiltonian \hat{V}_a can be expanded in the same way:

$$\hat{V}_a = \sum_{j+k+l+m=3} h_{a,jklm} h_x^{+j} h_x^{-k} h_y^{+l} h_y^{-m}. \quad (3)$$

For the third-order RDTs of one-period map, we have $h_{jklm} = \sum_{a=1}^N h_{a,jklm}$. The build-up fluctuation $h_{1 \rightarrow t, jklm} \equiv \sum_{a=1}^t h_{a, jklm}$ shows the accumulated RDTs from s_0 to the t -th sextupole.

For the case of multiple periods, the accumulated RDTs from s_0 to t -th sextupole in the $(u+1)$ -th period is:

$$\begin{aligned} \sum_{a=1}^{uN+t} h_{a, jklm} &= \sum_{a=1}^{uN} h_{a, jklm} + \sum_{a=uN+1}^{uN+t} h_{a, jklm} \\ &= \sum_{a=1}^N h_{a, jklm} \frac{1 - e^{iu\mathbf{m} \cdot \boldsymbol{\mu}}}{1 - e^{i\mathbf{m} \cdot \boldsymbol{\mu}}} + \sum_{a=1}^t h_{a, jklm} e^{iu\mathbf{m} \cdot \boldsymbol{\mu}} \\ &= \frac{\sum_{a=1}^N h_{a, jklm}}{1 - e^{i\mathbf{m} \cdot \boldsymbol{\mu}}} - \left(\frac{\sum_{a=1}^N h_{a, jklm}}{1 - e^{i\mathbf{m} \cdot \boldsymbol{\mu}}} - \sum_{a=1}^t h_{a, jklm} \right) e^{iu\mathbf{m} \cdot \boldsymbol{\mu}}, \end{aligned} \quad (4)$$

where $\mathbf{m} = (j - k, l - m)$ is the mode of resonance and $\boldsymbol{\mu} = (\mu_x, \mu_y)$ is the phase advances of one period. The third-order RDT build-up fluctuation can be written in the form of $C_{0, \mathbf{m}} + C_{t, \mathbf{m}} e^{iu\mathbf{m} \cdot \boldsymbol{\mu}}$, which is a circle in the complex plane when u is a variable. And $C_{t, \mathbf{m}}$ is dependent on the sextupole index t , so the build-up fluctuation of the RDT h_{jklm} is a series of concentric circles in the complex plane.

The second kind of RDT fluctuations shows the period map observed at different longitudinal positions. And we can measure it on a real machine. In order to measure the RDTs, we need another transformation to find the nonlinear invariants [4]:

$$e^{-iF} e^{i\mathcal{H}} R e^{iF} = e^{i\mathcal{H}} \mathcal{R}, \quad (5)$$

where \mathcal{H} is the phase-independent Hamiltonian in normal forms, and F is such a transformation. When the observation position s is between n -th and $(n+1)$ -th sextupole, the third

* baizhe@ustc.edu.cn

[†] fenggy@ustc.edu.cn

LONGITUDINAL BEAM DYNAMICS DESIGN FOR SUPER TAU-CHARM FACILITY

Linhao Zhang^{*}, Tao Liu, Sangya Li, Jingyu Tang[†], and Qing Luo[‡]
University of Science and Technology of China, 230026, Hefei, Anhui, China

Abstract

The project of Super Tau-Charm Facility (STCF) proposed in China, as a new-generation high-luminosity e⁺/e⁻ collider in the low-energy region with the center-of-mass energy of 2–7 GeV, is well underway. The luminosity is targeted at $1.0 \times 10^{35} \text{ cm}^{-2}\text{s}^{-1}$ at the optimized beam energy of 2 GeV. Longitudinal beam dynamics becomes of great importance for the STCF due to the constraints from the novel beam-beam effect called coherent X-Z instability and severe beam collective effects. In this paper, we will develop an iterative optimization model for the STCF longitudinal beam dynamics design, which takes into account the influence of transverse dynamics, coherent X-Z instability, and collective effects.

INTRODUCTION

The STCF proposed in China is a new-generation super high luminosity e⁺/e⁻ collider in the low-energy region spanning the center-of-mass energy of 2–7 GeV. It aims to explore the rich physics in the tau-charm energy range and even search for new physics beyond the standard model [1]. The goal luminosity of STCF reaches $1.0 \times 10^{35} \text{ cm}^{-2}\text{s}^{-1}$ at the optimized beam energy of 2 GeV, which is two orders of magnitude higher than that of the existing e⁺/e⁻ collider in the tau-charm field in China, BEPCII.

To achieve such high luminosity, a large Piwinski angle combined with the crab-waist collision scheme has been widely recognized as an effective approach [2], and adopted in the new-generation e⁺/e⁻ colliders such as SuperKEKB [3], BINP-SCTF [4], FCC-ee [5], and CEPC [6], etc. On one hand, through introducing a large Piwinski angle ϕ , the vertical beta function at the interaction point (IP) β_y^* can be squeezed into the level of effective bunch length σ_z/ϕ , to significantly raise the luminosity; On the other hand, the synchro-betatron coupling resonance introduced by the large Piwinski angle can be suppressed by the crab-waist correction scheme using crab sextupoles properly positioned on both sides of the IP. However, this scheme will introduce a novel beam-beam effect called coherent X-Z instability [7], which imposes stringent constraints on the longitudinal beam dynamics by requiring the horizontal beam-beam parameter ξ_x to be much less than the synchrotron tune ν_z .

Furthermore, the STCF is characterized by the beam properties of low energy, small emittance, high bunch intensity and large bunch numbers, which means that the

STCF faces significant beam collective effects. This also places strict limitations on the longitudinal parameters such as bunch length and energy spread.

Therefore, special attention is paid to the longitudinal beam dynamics design for STCF in this paper, which requires iterative optimization with transverse dynamics, beam-beam effects, and collective effects, etc., in order to search for possible optimal solutions.

DESIGN CONSIDERATIONS

The following are the specific considerations and requirements.

Luminosity

For fully symmetric flat electron-positron beam collisions, the relationship between luminosity and the associated parameters is illustrated in Fig. 1. One can see that the luminosity L is closely related to total beam current I , vertical beta function at IP β_y^* , vertical beam-beam parameter ξ_y , and hourglass factor F_h that is always less than 1. To achieve the goal luminosity of $1.0 \times 10^{35} \text{ cm}^{-2}\text{s}^{-1}$ at the optimized beam energy of 2 GeV, the beam current of 2 A and submillimeter β_y^* of 0.6 mm are first identified, which suggests that ξ_y is at least larger than 0.07 assuming F_h to be 1. This also implies a limitation on the bunch length σ_z since ξ_y is inversely proportional to σ_z under a large Piwinski angle ϕ with the total crossing angle of $2\theta = 60 \text{ mrad}$. Additionally, it is noted that the time resolution at the detector requires σ_z not larger than 12 mm.

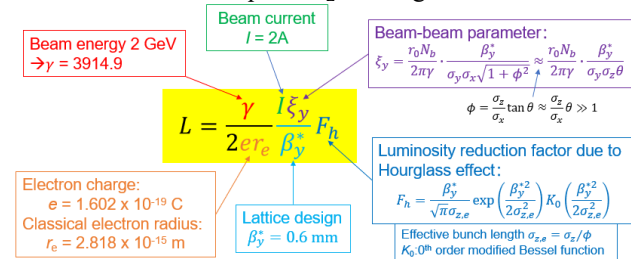


Figure 1: Luminosity and the correlated parameters.

Coherent X-Z Instability

Coherent X-Z instability, as a newly discovered coherent beam-beam interaction under a large Piwinski angle, primarily leads to an increase in the horizontal emittance ϵ_x [8]. Considering the coupling between horizontal and vertical emittances, it eventually results in an increase in the vertical emittance ϵ_y and thus a collapse of the luminosity. This instability cannot be suppressed through beam feedback systems but can only be avoided through appropriate parameter optimization. Typically, a stringent

^{*} zhanglinhao@ustc.edu.cn

[†] jytang@ustc.edu.cn

[‡] luoqing@ustc.edu.cn

DEVELOPMENT STATUS OF BEAM DYNAMICS SOFTWARE APES FOR CEPC*

Weibin Liu^{†1}, Yuan Zhang¹, Tianmu Xin, Zhe Duan, Zhiyuan Li¹,
Yaliang Zhao, Huiping Geng, Mengyu Su¹, Yixian Dai¹, Xiaohan Lu, IHEP, Beijing, China
¹also at UCAS, Beijing, China

Abstract

The physical design and beam dynamics study of the Circular Electron Positron Collider (CEPC) is an unprecedented challenge. In the simulation studies to evaluate its performance limitations and mitigation, the cross-talk between many physical phenomena must be properly modelled, including the crab-waist collision scheme with a large Piwinski angle, strong nonlinear effects, the energy sawtooth, beam-beam interactions, machine impedances, etc. To address this challenge, a software project APES was proposed in 2021 and received support from the IHEP Innovative Fund in 2022. The progress of the APES project are described in this paper.

INTRODUCTION

The CEPC was first proposed as a circular Higgs factory in 2012 and the conceptual design report was published in 2018 [1]. FCC-ee is a similar project proposed in CERN. During the design of these future colliders, the beam lifetime limitation due to the beamstrahlung effect, the synchrotron radiation induced by collision leading to a bunch lengthening and an increase in the beam energy spread, has been found and studied [2]. Different from conventional colliders, not only the transverse beam size, but also the longitudinal dynamics would be clearly influenced by the collision. That is why the 3D flip-flop instability may appear in CEPC or FCC-ee [3].

There would also be strong synchrotron radiation in the arc bending magnets of the machines, leading to a substantial “sawtooth”-shape variation of the central beam energy along the ring, which is the so-called sawtooth effect. The magnet tapering method has been proposed to mitigate this effect [4]. This requires new optics calculation method to consider the energy change along the ring.

After the crab-waist scheme was proposed around 2006 [5], the new collision scheme has become the baseline design for the following high performance circular e+e- colliders. However sub-millimeter scale β_y^* in future machines would induce strong lattice non-linearity and a very small dynamic aperture. During the lattice design and optimization, it has been found that the short-term dynamic aperture tracking could not predict the long-term beam lifetime [6].

In recent years, a new horizontal coherent beam-beam instability (X-Z instability) has been found [7]. The following simulation and analysis also show that the potential-well distortion effect would impact the behaviour of X-Z instability

clearly [8,9]. This tells us the cross-talk between beam-beam and longitudinal impedance could not be ignored.

Apart from these novel effects uncovered in the design study of CEPC and FCCee, the commissioning of SuperKEKB also reveal that there is still a gap in the modelings and simulations to explain and mitigate the difficulties in the practical machine tunings [10]. These have told us that the beam dynamics of future e+e- colliders would be very challenging.

A beam dynamics software project “APES” (Accelerator Physics Emulation System) has been proposed, with an objective to address the beam physics issues in CEPC in a unified, extendable manner:

- The modeling of the collider, especially the complicated interaction region and the cross-talk of common hardware shared by the two rings.
- Lattice design and performance evaluation, including symplectic tracking, optics calculation/matching, emittance calculation, modeling of the sawtooth and tapering effect, analysis of nonlinear optics performance, spin dynamics evaluation, machine error effects and correction algorithms, multi-objective optimization etc.
- Performance evaluation/prediction of the collider, the cross-talk between realistic lattice, beam-beam interaction, spin, collective effects and necessary hardware modeling.
- Interface with detector (MDI) and machine protection (particle-matter interaction), easy access and interaction with software dedicated for these purposes.

These functionalities and features will empower users to design, analyze, and optimize accelerator systems with greater accuracy and efficiency. Additionally, we can foresee several potential applications when these capabilities have been fully developed:

- Tracking simulations to evaluate the luminosity and beam lifetime with the realistic lattice and the strong-strong beam-beam interaction, as well as impedance effects.
- Simulations of the injection process, to evaluate the injection efficiency in the presence of machine imperfections, beam-beam interaction and impedance effects, and to prepare beam loss information for the design of collimators and evaluation of the influence to the detectors.

* Work supported by IHEP Innovative Fund

[†] liuw@ihep.ac.cn

PHYSICAL DESIGN FOR EEHG BEAMLINES AT S³FEL

Li Zeng, Xiaofan Wang*, Yifan Liang, Huaiqian Yi, Weiqing Zhang^{1†}, Xueming Yang²

Institute of Advanced Science Facilities, Shenzhen, China

¹also at Dalian Institute of Chemical Physics, CAS, Dalian, China

²also at Southern University of Science and Technology, Shenzhen, China

Chao Feng, Zhen Wang

Shanghai Advanced Research Institute, CAS, Shanghai, China

Yong Yu, Jitao Sun, Xinxing Li

Dalian Institute of Chemical Physics, CAS, Dalian, China

Abstract

The proposed Shenzhen Superconducting Soft X-Ray Free-electron Laser (S³FEL) aims at generating FEL pulses from 1nm to 30nm. At phase-I, two undulator beamlines work at echo-enable harmonic generation (EEHG) principle. The two undulators will cover the spectral ranges 2.3-15 nm (~ 83-539 eV) and 5-30 nm (~ 41-248 eV), respectively, when receiving electrons from 2.5 GeV superconducting linac. However, the generated FEL radiation is sensitive to various electron beam properties, e.g., its energy profile influenced by collective effects such as Coherent Synchrotron Radiation (CSR), especially at high harmonics. To generate intense full coherent FEL radiation at ultra-short wavelength, a novel technique of EEHG cascaded harmonic lasing method is also considered. Physical design and FEL performance are described in this paper.

INTRODUCTION

The proposed Shenzhen Superconduction Soft X-Ray Free-electron Laser (S³FEL) [1] is a high repetition rate FEL facility that consist of a 2.5 GeV CW superconducting linac and four initial undulator lines, which aims at generating X-rays between 40 eV and 1 keV at rates up to 1 MHz.

Two undulator beamlines (FEL-3 and FEL-4) work at echo-enable harmonic generation (EEHG) [2] principle which has the major advantage of full coherence, precisely arrival time control, uniform longitudinal profile and so on. The shortest wavelength is about 2.3 nm at a harmonic over one hundred. Since the various collective effects, the degrading of FEL performance becomes severer at such high harmonic number. One possible solution is adapting a novel technique called EEHG cascaded harmonic lasing method. This paper presents the detailed FEL simulation results for start-to-end electron beam coming from the superconducting linac.

FEL PERFORMANCE

The basic electron beam parameters after linac are listed in Tabel 1. The slice parameters of the start-to-end electron beam are shown in Fig. 1. The core of the bunch has rela-

tively flat energy and current with normalized emittance of about 0.5 mm-mrad.

Table 1: Electron Beam Parameters

Parameter	Value	Unit
Beam energy	2.5	GeV
Slice energy spread	200	keV
Peak current	800	A
Charge	100	pC
Normalized emittance	0.5/0.5	mm·mrad

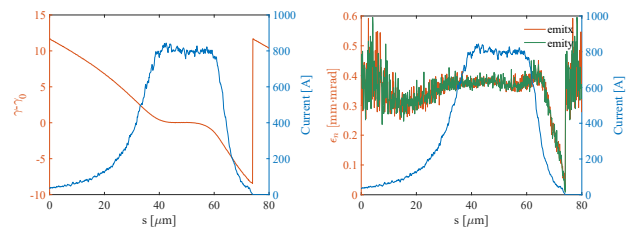


Figure 1: Beam energy (left), normalized emittance (right) and current (blue) of the electron beam.

The parameters of undulator beamlines and seed lasers are listed in Table 2. The FEL simulations are performed with electron beam after corresponding beam transport line and carried out by the time-dependent mode of GENESIS [3].

Table 2: Undulator Beamlines, Seed Lasers (SL) Parameters

Parameter	FEL-3	FEL-4
FEL wavelength [nm]	2.3-15	5-30
Undulator type	PMU	PMU+EPU
Undulator period [mm]	43	50
SL wavelength [nm]	266.7/240-267	266.7/240-267
SL pulse length [fs]	100	100
SL peak power [MW]	>200	>200
SL Rayleigh length [m]	1.0	1.0

FEL-3 (EEHG, 2.3–15 nm)

FEL-3 generates FEL radiation from 2.3 nm to 15 nm, covering the entire water window (2.3-4.4 nm).

* wangxf@mail.iasf.ac.cn

† weiqingzhang@dicp.ac.cn

A SCHEME OF FULLY COHERENT X-RAY FREE ELECTRON LASER FOR THE SHINE BASED ON FRESH-SLICE

Y. X. Liu[†], T. Liu

Shanghai Institute of Applied Physics, Chinese Academy of Sciences Shanghai, China
University of Chinese Academy of Sciences, Beijing 100049, China
Shanghai Advanced Research Institute Chinese Academy of Sciences, Shanghai, China

Abstract

In this paper, the fresh-slice self-seeding free electron laser scheme is studied, and the feasibility of its application in the SHINE project is analyzed. The scheme used the fresh-slice method to generate the beam with adjustable spatial distribution, which can effectively improve the longitudinal coherence and stability of the self-seeding output radiation. Through the FEL simulation, we demonstrated that this scheme can produce a highly stable, narrow bandwidth pulse output under the SHINE's parametric conditions, which will be beneficial to further improve the performance of this device in the future.

INTRODUCTION

Conventional SASE pulses originate from stochastic noise and are essentially random [1], which significantly affects the stability and output power of the self-seeding FEL. However, when a self-seeding scheme generates FEL using an ultra-short, high-current electron beam with a specific duration [2], the level of fluctuations can be reduced to a few percent while also maintaining a temporally coherent FEL output, resembling an ideal laser or an external-seeded FEL.

The fresh-slice method, also paving the way to very high peak power and high brightness XFEL pulses [3], uses either two different electron bunches or two single bunch slices, one to generate the seed signal and the other to amplify it in a tapered undulator to very high peak power. The method effectively eliminates the compromise between the seed power at the monochromator exit and the energy spread of electron slices within the seeded undulator section [4], thereby enhancing electron capture and reducing susceptibility to sideband instability [5].

Using the fresh-slice method to enhance the stability and power of self-seeding is an extremely appealing choice, while the SHINE project focuses on studying self-seeding FEL schemes covering the 5-15 keV hard X-ray range [6]. The changes to the self-seeding approach would contribute to improve the future performance of the SHINE. In this manuscript, we will demonstrate the simulation results of a bunch with high-current head using the fresh-slice method, which will provide some insights for the design of SHINE in the future.

* Work supported by the CAS Project for Young Scientists in Basic Research (YSBR060), the Shanghai Natural Science Foundation (23ZR1471300), and the CAS-Helmholtz International Laboratory on Free Electron Laser Science and Technology (HZXM2022500500).

[†] email address: liuyixuan@sinap.ac.cn.

FRESH-SLICE SELF-SEEDING

A schematic of the fresh-slice self-seeding used in the simulation is shown in Fig. 1. Selectively lasing with different slices of the electron beam is achieved with the fresh slice method. The electron bunch experiences a head-tail transverse kick by the wakefield generated in the D1 dechirper, set to an offset from the machine axis. Before the initial undulator phase, orbit correctors are utilized to direct the bunch into a head-lasing orbit. A saturated photon pulse is produced in the first section of the high-current bunch head. Then the photon pulse transmits from the diamond monochromator and generates a narrow bandwidth portion of it that is diffracted. The transmitted X-ray pulse presents a short, wide-bandwidth pulse followed by a stable, long, narrow-bandwidth tail. The chicane is used to delay the electron bunch tail such that it is overlapped with the narrow-bandwidth tail of the photon pulse. The bunch orbit is switched to a tail-lasing one around the chicane, and the monochromatic seed is amplified by the fresh electrons on the bunch tail in the second undulator section.

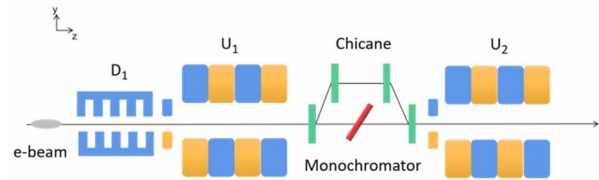


Figure 1: Schematic layout of the proposed scheme based on fresh slices.

Beam Parameters

Based on the proposed scheme, FEL simulations were performed using the code Elegant [7] and Genesis 1.3 [8]. The overall electron beam parameters and radiation parameters used in the simulations are presented in Table 1.

Table 1: Electron Beam and Radiation Parameters

Parameter	Value	Unit
Beam energy	8	GeV
Energy spread	0.01	%
Normalized emittance	0.5	mm · mrad
Undulator period	2.6	cm
Undulator strength K	1.3415	-
FEL wavelength	0.1	nm

INVESTIGATION ON THE TRAPPED MODES OF CPMU AT HEPS

Sen Yue ^{*}, Na Wang [†], Saike Tian, Jintao Li
Institute of High Energy Physics, [100049] Beijing, China

Abstract

The Cryogenic Permanent Magnet Undulator (CPMU) is a crucial component in synchrotron radiation sources. Due to the small magnet gap of CPMU, the interaction between the beam and its surroundings is strong, which can result in a significant contribution to coupling impedance. In this work, the influence of CPMU on coupling impedance was investigated using wakefield and eigenmode solvers. The results indicate that some of the transverse impedance resonances in CPMU were much stronger than the impedance threshold determined by synchrotron radiation damping, which could cause vertical beam instability. To address this issue, different types of damping materials were investigated through simulations to suppress the resonances.

INTRODUCTION

The in vacuum undulator (IVU) is a device, whose magnet is put inside in the vacuum box, and thus the magnet gap can be designed as much small as possible [1]. CPMU is a kind of undulator, whose magnet is working at cryogenic. Compared with IVU, it can provided a stronger magnetic at the same magnet gap, which can help to increase the frequency of synchrotron radiation generated by electron beams.

Due the small gap, the interaction between beam and its surroundings can be strong. Recently, multiple light sources, such as the Canadian Light Source [2], the Australian Light Source [3], and SLAC's SPEAR3 [4], have all discovered beam instability phenomena caused by the trapped mode inside the IVU.

In the first phase of the High Energy Photon Source (HEPS) project, 6 CPMUs will be installed in the storage ring. The CPMU have a longitudinal length of approximately 2.6 m, with a standard magnet gap of 5 mm. Therefore, the evaluation of its influence on beam is crucial to ensure the stable operation of the beam within the storage ring.

VERTICAL IMPEDANCE

Due to limited computational resource, the three-dimensional model of CPMU need to be simplified. Its unnecessary detailed structures were removed, and the length of mangnet was reduce to 1 m, to reduce the mesh number for a short simulation time. Figure 1 shows the simplified model, and the right figure depicts the transverse cross section of CPMU, which similar to a circular ridge waveguide.

Compared to circular waveguide, the ridge waveguide has a lower cutoff frequency. As the size of beam pipe is large compared to the magnet gap, the cutoff frequency formed

by the magnet and vacuum cavity is lower than that of the beam pipe. As a result, some modes with low-frequency can be trapped in CPMU, and it is also called as trapped modes.

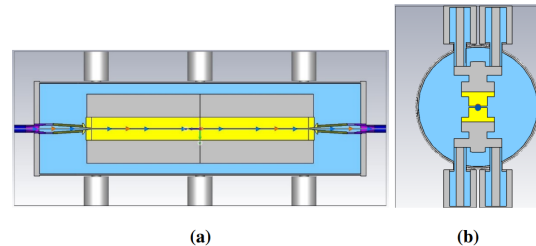


Figure 1: The simplified model of CPMU. (a): vertical cross section; (b): transverse cross section.

Through the CST wakefield solver, the vertical coupling impedance of the simplified model is shown in Fig. 2. In the simulation, the RMS length of the beam bunch was set to 100 mm, and the calculation length of the wakefield is 20 m.

Figure 2 shows that there are mainly two obvious impedance peaks at 96 MHz and 189 MHz. The real part impedance of these two peak are 2.1 and 0.6 M Ω /m, respectively. Due to these two peaks have a high Q factor, the wakefield is hard to convergence. Thus, the magnitude of the vertical impedance is smaller than expected value.

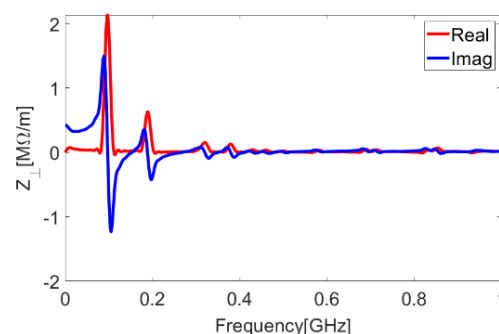


Figure 2: The vertical coupling impedance.

TRAPPED MODES

Although the CPMU model has been simplified, the simulation still takes nearly one month to obtain the impedance results in Fig. 2. As the simulation time is proportional to the wakefield length, it will require a large amount of time and computational resources, to obtain a converged result. Therefore, the eigenmode solver is adopted to analyze these two impedance peaks, which requires little computational resources and time.

^{*} yuesen@ihep.ac.cn

[†] wangn@ihep.ac.cn

MULTI-BUNCH OPERATION MODE FOR SIMULTANEOUSLY SERVING SASE AND SEEDING FEL BEAMLINES

Yifan Liang, Xiaofan Wang*, Li Zeng, Huaqian Yi, Weiqing Zhang^{1†}, Xueming Yang^{1,2}

Institute of Advanced Science Facilities, Shenzhen, China

¹also at Dalian Institute of Chemical Physics, CAS, Dalian, China

²also at Southern University of Science and Technology, Shenzhen, China

Yong Yu, Jitao Sun, Xinmeng Li

Dalian Institute of Chemical Physics, CAS, Dalian, China

Abstract

Modern free-electron laser (FEL) facilities are designed to simultaneously serve multiple undulator lines to provide x-ray pulses with high peak power and tunable wavelengths. To satisfy different scientific demands, it is preferred to make the separate undulator lines work under different FEL schemes, such as the self-amplified spontaneous emission (SASE) scheme and the echo-enabled harmonic generation (EEHG) scheme. However, different FEL schemes have different requirements on the beam longitudinal distribution. Here, we propose to use multiple bunches to simultaneously serve the undulator lines and put the bunches at different acceleration phase to change the bunch length with two compressor chicanes. The acceleration phase for each bunch is varied by adjusting the time delays of the photocathode drive laser pulses with the accelerator settings unchanged. The start-to-end simulation demonstrates that a fs bunch with high peak current can be produced to serve the SASE line while a bunch with hundred-of-fs length and uniform current distribution can be produced to serve the EEHG line. The FEL performances are simulated and discussed.

INTRODUCTION

Modern FEL facilities are designed to operate two or more undulator lines simultaneously with a single-pass linac-based machine and exploit beam distribution systems to send electron bunches to their respective beamlines. In normal conducting linacs, limited by the low repetition rate, only a modest average brightness can be provided. It is necessary to accelerate two electron bunches in the same radiofrequency (RF) macropulse to increase the repetition rate, as in SwissFEL [1]. In superconducting RF linacs, megahertz (MHz) electron bunches can be provided and the photon average brightness is greatly enhanced. The MHz electron bunches are then sent to different undulator lines in a group mode as in European XFEL [2] and FLASH [3] or one by one as in LCLS-II [4] and SHINE [5].

To extend the application range of FEL generated light, it is preferred to operate different undulator lines under different schemes to provide either sub-fs or fully longitudinally coherent pulses. However, different FEL schemes have different requirements on the beam longitudinal

distribution. The SASE scheme requires fs electron bunch with high peak current to shorten the saturation length and increase the peak power, while seeding schemes require bunches with hundred-of-fs length and uniform current distribution to improve the modulation stability. To satisfy the requirements of different FEL schemes, one solution is to accelerate the bunches at different accelerating phases and change the bunch lengths with compressor chicanes. The acceleration phase for each bunch can be varied by changing the microwave amplitude and phase as has been done in SwissFEL [1] and FLASH [6]. However, in superconducting RF linacs with MHz repetition rate of macropulses, changing the amplitude and phase of different macropulses is a challenge and might affect the machine stability.

In this paper, we study the multi-bunch scheme and change the acceleration phase of each bunch by adjusting the time delays of the photocathode drive laser. A bunch with hundred-of-fs length and uniform current distribution is produced for EEHG lasing while a sub-fs bunch with high peak current can be produced for SASE lasing under the same machine parameters.

MULTI-BUNCH SCHEME

The multi-bunch scheme has been studied both theoretically and experimentally [7-10]. Here, we concentrate on modulating the longitudinal distribution of the bunches into different shapes to simultaneously maximize the radiation performance of different FEL schemes in different undulator lines. We take the typical two-stage compression beamline at S3FEL as an example, as shown in Fig. 1. Laser pulses with a repetition rate of 1 MHz illuminate the photocathode to produce electron bunches. Two chicanes are used to compress the bunch length from several picoseconds to tens of femtoseconds. After acceleration to 2.5 GeV, the bunches are distributed to separate undulator lines respectively. Two of the undulator lines exploit the SASE scheme to lase and the other two exploit the EEHG scheme. To simultaneously maximize the radiation performance of all the undulator lines, the bunches directed into different undulator lines are put on different acceleration phase and thus different compression just by changing the time delay of the photocathode laser pulses.

Injector

The injector includes a normal-conducting continuous-wave (CW) RF gun operating at 217 MHz (6th sub-

Email address: *wangxf@mail.iasf.ac.cn

†weiqingzhang@dicp.ac.cn

PHYSICAL DESIGN OF AN S-BAND COLD CATHODE RF GUN*

Tian Hui He[†], Hanxun Xu, Kui Zhou, Zheng Zhou

Institute of Applied Electronics, Chinese Academy of Engineering Physics, Mian Yang, China

Abstract

In recent years, the properties of new field emission materials have been gradually improved with the advancement of materials research fields, which have provided the possibility for the research and realization of cold cathode microwave electron guns. A 0.32+1 cell S-band microwave electron gun was designed based on the emission properties of carbon nanotube films and ultra nano diamond films. This article mainly introduces the selection of electron gun cavity, RF design and corresponding thermal analysis. The physical design results basically meet the design requirements.

INTRODUCTION

With the continuous advancement of accelerator technology, radio frequency guns are also iteratively developed from generation to generation, from the original hot cathode RF gun to the now widely used photocathode RF gun. The hot cathode RF gun has a large beam intensity and serious electronic backlash; Although the photocathode RF gun has good beam quality, the current intensity is not large, and additional costs are required for the laser. At present, with the advancement of material technology, the use of cold cathode is gradually increasing, cold cathode RF gun because of its beam quality is relatively good, the current intensity is large, and does not require additional filament heating power supply and laser, low cost, compact structure, so as to be expected by more and more institutes. Based on the emission characteristics of diamond film cathode [1] and carbon nanotube cathode [2] described in the existing literature, a 0.32+1 cell S-band cold cathode RF gun is designed.

The cold cathode is based on the principle of field-induced emission, and the distribution of field-induced emission current density in the microwave field is similar to the Gaussian distribution on time scales [3].

$$J(t) = J_0 e^{-C \frac{\phi^{3/2}}{\beta E_0} \frac{(\omega t - \pi/2)^2}{2}} \quad (1)$$

Its rms width is:

$$\sigma = \sqrt{\beta E_0 / (C \phi^{3/2})} \quad (2)$$

In the microwave field, the maximum value of the field-induced emission current distribution is exactly in the middle of the positive half-period of the microwave field, and since the area occupied by $\pm 2\sigma$ accounts for 95% of the total area of the Gaussian distribution, it can be considered that the width of the field-induced emission is $\pm 2\sigma$.

* Work supported by Infrared terahertz free electron laser device project
[†] htth111@163.com

CAVITY TYPE SELECTION

The general cold cathode RMS width σ is about 15° , and its emission width in the microwave field is about $\pm 2\sigma$, that is, $-30^\circ \sim 30^\circ$. An emission phase width of 60° will inevitably lead to electron back burst when the field strength of the cathode plane is not large enough. In order to avoid back bombardment, there are two solutions to the design of the first cavity, one is to reduce the length of the first cavity, and the other is to increase the cathode surface field strength. The problem with reducing the length of the first cavity is that the maximum field strength in the first cavity is offset and concentrated on the platter, and the length of the first cavity is too short, which increases the difficulty of processing and commissioning. Increasing the field strength of the cathode surface leads to a sharp increase in the emission phase width for the field-induced emission cathode, making the field-induced emission similar to the hot cathode emission. At present, the opening electric field of nitrogen-doped diamond film cathode is generally about 10 MV/m, and the opening electric field of carbon nanotube cathode is lower, generally 48 MV/m, and its maximum emission electric field is about 20 MV/m, which will inevitably lead to back bombing. Therefore, the only alternative method at present is to reduce the length of the first cavity.

Assuming that the field-induced emission RMS width σ is 15° , the relationship between the minimum field strength required for the last emitted electron at 30° overflows the first cavity and the length of the first cavity, as shown in Fig. 1. As can be seen from the figure, the shorter the first cavity, the smaller the minimum field strength required for the end electrons to overflow the first cavity. Under the cathode

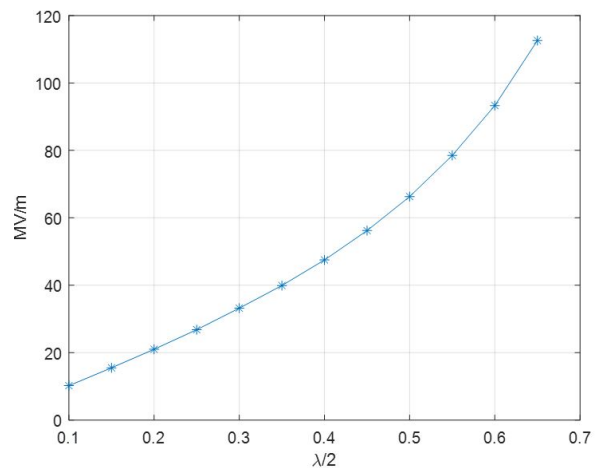


Figure 1: The relationship between the minimum field strength of the cathode plane required for the end electron overflow the first cavity and the length of the first cavity.

STUDIES ON BEAM INJECTION SYSTEM FOR WUHAN ADVANCED LIGHT SOURCE STORAGE RING

Y. Zou[†], H. H. Li, Y. Chen, J. H. He, IAS, Wuhan University, Wuhan, China

Abstract

Wuhan Advanced Light Source is the low-energy 4th generation advanced light source, which is proposed by Wuhan University, China. It includes a 1.5 GeV full-energy LINAC injector, a 180 m circumference, 1.5 GeV low-emittance storage ring, and a series of state-of-the-art beam lines. The standard 7BA magnetic focusing structure is adopted for the storage ring to lower the beam natural emittance and the lattice has been well-designed and optimized by multiple-objective genetic algorithm to maximize the dynamic aperture and energy acceptance. The dynamic aperture of the storage ring at injection can reach up to 8 mm in the horizontal plane, which makes the off-axis beam injection method possible. An off-axis beam injection scheme based on the pulsed nonlinear magnet is to be employed for the storage ring. Detailed studies about the beam injection scheme, including the beam optical design, nonlinear magnet design and optimization, have been performed and multi-particle simulations have also been carried out to study the beam injection procedure.

INTRODUCTION

Wuhan Advanced Light Source (WALS) project was proposed by Wuhan University in 2016 [1], of which the accelerator includes a 1.5 GeV full-energy LINAC injector, and a 180 m circumference of low-emittance storage ring. The ring lattice is 8-fold symmetrical structure, of which each cell includes a hybrid 7BA structure and a 6.8 m of long straight section. The horizontal nature emittance is around 214 pm rad. Several measures have been taking into account to reach this target, e.g., employing bending magnets with both transverse and longitudinal gradients; employing two groups of the reverse dipoles, etc. A superbend magnet, of which the peak field strength reaches as high as 3.57 T, is adopted in the center of each cell to expand the application boundaries of the synchrotron radiation light source to the field of hard X-ray. Both permanent and electro-magnets are used in the storage ring. A series of sextupoles are employed at high dispersion zone to correct the chromaticity with moderate strength. Nonlinear effects would be introduced in the ring by sextupoles, which would reduce the dynamic aperture and momentum acceptance that need to be addressed. The multiple-objective genetic algorithm (MOGA) is introduced to optimise the lattice design in order to obtain the maximum dynamic aperture and energy acceptance. Two of the eight straight sections are reserved for beam injection system and RF system, respectively. Beam injection system is to bend the electron beam into the storage ring while RF system is to supplement the electron energy loss and stretch the bunches in the ring to increase the beam lifetime. The other straight

sections are reserved for insertion devices. Figure 1 shows one eighth of the lattice and Twiss parameters for the WALS storage ring while Table 1 shows the main parameters.

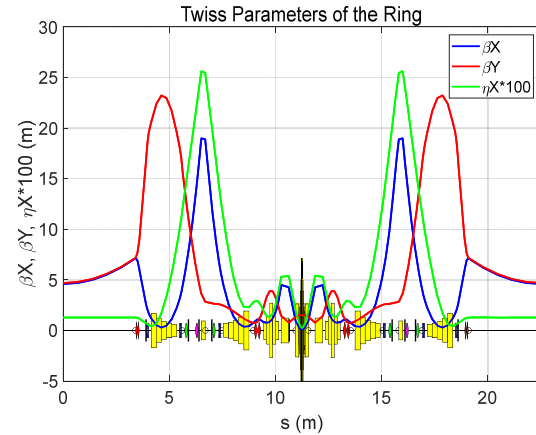


Figure 1: One eighth of the lattice and Twiss parameters for the WALS storage ring.

Table 1: the Main Parameters of the Storage Ring

Parameter	Value
Energy (GeV)	1.5
Beam current (mA)	500
Circumference (m)	180
Revolution period (ns)	600
Harmonic number	300
Horizontal emittance (pm rad)	214.8
Damping time H/V/S (ms)	7.08/17.02 /28.52
Betatron tunes Hor./Ver.	20.279/10.190
Energy acceptance (%)	4.2
Momentum compact factor	0.00036
Radiative loss per turn (keV)	105.9
Synchrotron phase (deg)	169.8
Bunch length (ps)	16.37

BEAM INJECTION SCHEME

The beam injection system is employed to bend the electron beam into the storage ring. Since the beam dynamics aperture is relatively large, the off-axis accumulate injection scheme is available. The philosophy of injection system design is to seek high injection efficiency while being transparent to the storage beam. The traditional off-axis injection is normally implemented by a local bump formed by two groups of bump magnets. This method needs a relatively long injection straight section and the local bump is difficult to be fully closed mainly due to the fields error of the bump magnets. An alternative off-axis injection method based on pulsed nonlinear magnet (PNM) was firstly introduced at KEK [2, 3], and has been well studied and implemented at several facilities, e.g., BESSY [4],

[†] Email address: ye.zou@whu.edu.cn

START TO END SIMULATION FOR A COMPACT THz-FEL *

Ruiying Luo, Qushan Chen[†]

State Key Laboratory of Advanced Electromagnetic Engineering and Technology,
 Huazhong University of Science and Technology, Wuhan, China

Abstract

An oscillator type terahertz free electron laser (THz-FEL) is under construction at Huazhong University of Science and Technology (HUST). The designed electron beam energy ranges from 8 MeV to 14 MeV, and the radiation frequency ranges from 3 THz to 10 THz. FEL requires high quality electron beams of emittance, energy spread, bunch charge etc. To know the overall facility performance, a start-to-end simulation (from electron gun to the end of the oscillator) of the THz-FEL is performed. The simulation of the electron gun to the exit of the linac is performed using PARMELA, where the effect of space charge effects is considered. In addition, the effect of beam loading effect is considered for the linac. The transport line is matched and simulated using ELEGANT. GENESIS 1.3 and OPC is used for the lasing process. Results of the simulation are presented and discussed in this paper.

INTRODUCTION

Terahertz (THz) radiation has attracted more and more attention because it holds the promise of enabling various new scientific and industrial applications. Due to the advantages of high output power, continuously adjustable wavelength, etc, terahertz free electron laser (THz-FEL) has received wide attention and research [1–3]. Huazhong University of Science and Technology (HUST) has constructed a compact oscillator type THz-FEL facility. It mainly consists of an injector and laser. The injector provides the required electron beam, which mainly includes EC-ITC (external cathode and independently tunable cavities) RF (radio frequency) gun, an S-band traveling wave (TW) linac and a double bend achromatic transport line. The laser consists of a pure permanent magnet type undulator and an optical resonant cavity [4]. The layout of HUST THz-FEL is depicted in Fig. 1.

Start-to-end simulation is an important method to understand the performance of FEL. It can take nonlinear effects into account and provide guidance for FEL design and optimization. To know the overall facility performance, a start-to-end simulation is performed. PARMELA is used to simulate the electron gun and linac, where the space charge effect is considered. ELEGANT is used to match and simulate the transport line. GENESIS 1.3 is used to simulate the interaction of the electron bunch with the radiation field in the undulator. And OPC is used to simulate the propagation of the radiation field in the optical cavity. In the paper, taking the beam energy of 14 MeV as an example, the parameters

of bunch at the entrance of the undulator is obtained and the performance of the radiation field is analyzed.

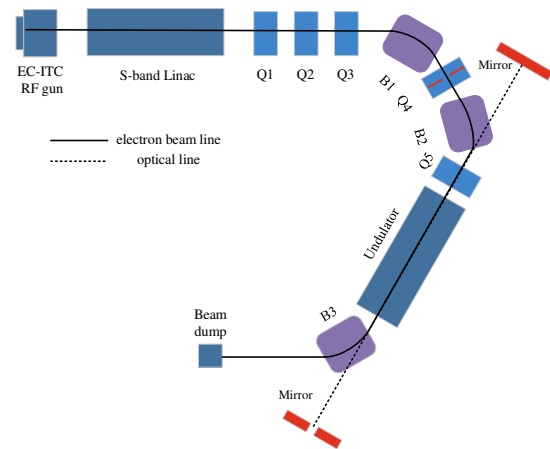


Figure 1: The layout of HUST THz-FEL.

MACHINE LAYOUT AND SET UP

The EC-ITC gun is composed of a thermionic cathode and two independently tunable cavities. The electrons are extracted from the thermionic cathode by using a high voltage of 15 kV and then injected into two cascaded, but independent tuning standing wave cells [5]. The two standing wave cells (C1 and C2) bunch the electron pulses into multiple electron bunches with an interval of 350 ps and accelerate the bunches to 2.6 MeV. The maximum gradients of C1 and C2 are 40 MV/m and 89 MV/m, respectively. The bunch at the exit of the electron gun has a long tail, which results in beam loss during acceleration and transport processes.

The TW linac operates at 2856 MHz and can accelerates the bunch from 2.6 MeV to 8-14 MeV to meet the requirements of the lasing frequency varying from 3 to 10 THz. Instead of using the typical coupling output structure at the end, it employs coaxial load absorbing cells [6]. The total length of the linac is 875 mm, and there are 24 cells in all, of which the last 4 cells are coaxial load absorbing cells. Since the electron bunch has a long tail, the tail particles will absorb microwave power when they enter the linac. Therefore, careful analysis of the beam loading effect is required to obtain the acceleratng gradient of each cell.

The transport line transports the bunch from the exit of the linac to the entrance of the undulator and makes the bunch with suitable Twiss parameters at the entrance of the undulator. The bunch has a long tail, and the tail particles belongs to useless particles. Therefore, an x-directional slit

* Work supported by National Natural Science Foundation of China (No.12175077)

[†] chenqushan@hust.edu.cn

BEAM DYNAMICS STUDY OF A PHOTO-INJECTOR AT WUHAN LIGHT SOURCE

Ze-Yi Dai, Yuan-Cun Nie[†], Zi Hui, Jian-Hua Zhong, Lan-Xin Liu, Zi-Shuo Liu, Jia-Bao Guan, Wei-Wei Zhou, Kai-Shang Zhou, Ji-Ke Wang, Yuan Chen, Ye Zou, Hao-Hu Li, Jian-Hua He^{††}
The Institute for Advanced Studies, Wuhan University, Wuhan 430072, China

Abstract

A photo-injector is under development at Wuhan Light Source (W HLS) to provide beams for the 1.5 GeV storage ring proposed as a fourth-generation synchrotron radiation light source and a future free electron laser (FEL) facility. The photo-injector and the following LINAC will be able to produce electron beams with low emittance (<2 mm·mrad), high bunch charge (~ 1 nC), small energy spread ($<0.5\%$), and short bunch length, which meet the requirements of the ring injection and the FEL operation simultaneously. The injector boosts the bunch energy to 100 MeV, which is mainly composed of a photocathode RF gun working at 2998 MHz, two solenoid coils for emittance compensation, and two 3-meter-long 2998 MHz traveling-wave (TW) accelerator units. Beam dynamics optimization of the photo-injector is presented in detail, which has been performed with multi-objective genetic algorithm (MOGA) combining theoretical analysis and ASTRA code. After optimization, the 95% projected transverse emittance has reached as low as 0.45 mm·mrad with an RMS bunch length of about 1.0 mm at a bunch charge of 1 nC. Such emittance is close to the intrinsic thermal emittance at the photocathode, implying that there is almost no emittance growth during beam transmission.

INTRODUCTION

Including the 4th generation diffraction-limited storage rings (DLSR) and FEL, WHLS is proposed to be built in Wuhan, Hubei Province of China. It is planned to construct a 1.5 GeV low-energy storage ring with emittance less than 230 pm·rad in stage I. A photo-injector is an ideal candidate to guarantee performance of the accelerator, which can provide high brightness electron beams at the source.

The photo-injector system at WHLS boosts the bunch energy to 100 MeV with high bunch charge and low emittance, which consists of a 1.6-cell normal conducting RF (NCRF) gun followed by two 3 m-long S-band accelerator units, and two solenoids placed at the exit of the gun and around the first accelerator unit, respectively. Such a design can produce electron beams with high bunch charge and low emittance, which is widely adopted in the similar facilities, such as MAX IV, HALF, LCLS, Pal-FEL, Swiss-FEL, etc. [1-5].

* Work supported by the Science and Technology Major Project of Hubei Province, China (2021AFB001).

[†] email address: nieyuncun@whu.edu.cn

^{††} email address: hejianhua@whu.edu.cn

BEAM DYNAMICS OPTIMIZATION WITH ASTRA CODE

Layout of the injector system is shown in Fig.1. The projected transverse emittance is determined by a large number of parameters, including transverse and longitudinal distribution of the driving laser pulse, field gradient and phase of the RF gun, magnetic field strength and profile excited by the solenoid coils, field gradient and phase of the S-band TW accelerator units, and locations of these hardwares. To find the global optimal solution, the multi-objective genetic algorithm (MOGA) combined with ASTRA code can be used [6,7]. However, before combination of the two tools, it is necessary to narrow down the scanning range of each parameter to accelerate convergence.

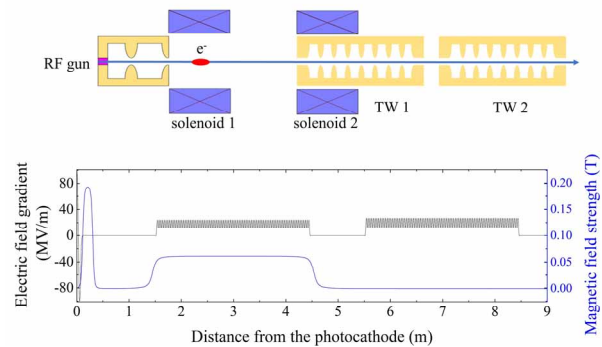


Figure 1: Layout of the photo-injector at WHLS.

The driving laser with temporal flat-top distribution and transversely truncated Gaussian distribution can linearize the space-charge effect [8]. According to experience, flat-top temporal distribution with a full-width-at-half-magnitude (FWHM) pulse length of around 10 ps and transversely about 1 sigma truncation of Gaussian distribution are selected in our simulation. The RMS transverse beam size can be calculated by $Q = \pi r^2 \epsilon E$, where E is the electric field during photoemission, r is the beam radius, ϵ is permittivity of vacuum, and Q is initial bunch charge. To obtain a bunch charge of 1 nC or even higher, Cs₂Te semiconductor photocathodes are preferred, which are widely used in photo-injectors with the advantage of high quantum efficiency (QE) and moderate lifetime. Operating RF field gradient in the gun should be as low as possible to prolong the photocathode lifetime. On the other hand, higher field gradient in the gun is profit for improving beam emittance. To make a compromise, the gradient was set to 100 MV/m. The intrinsic thermal emittance at the photocathode was set to 0.9 mm·mrad/mm.

COMPACT ACCELERATOR LIGHT SOURCE FOR INDUSTRIAL APPLICATIONS *

Q.L. Zhang ^{†1,2,3}, C.L. Li¹, K. Wang^{1,2,3}, Y.X. Wang^{1,2,3}, Y.J. Lu⁴

¹Shanghai Advanced Research Institute, CAS, Shanghai, China

² Shanghai Institute of Applied Physics, CAS, Shanghai, China

³ University of Chinese Academy of Sciences, CAS, Beijing, China

⁴ Zhangjiang Laboratory, Shanghai, China

Abstract

Synchrotron radiation has great application potential in industry. However, the large scale of modern light source has limited it from popular use. Compact accelerator light source has many virtues such as small scale, cost effectiveness, maintenance convenience, etc., which make it a main solution of light source application in industry. The idea has attracted great interests from many institutes, and much effort has been put into its research and development. In this paper we present a design of compact accelerator light source with very small scale. The lattice is very simple to ensure its compactness, while the beam parameters remain flexible to industry needs.

INTRODUCTION

Synchrotron radiation was considered as byproduct of colliders in the past and turned to be a powerful tool in scientific research after the discovery of its merits in light spectrum, brightness, polarization, collimation, etc. Light sources have been widely used as a large research platform for scientists, and numerous achievements have been made with the help of synchrotron radiation.

A light source typically consists of an injector, a storage ring, some beamlines and experiment stations. To satisfy the needs of users, light sources are usually built in a large scale to accommodate various types of beamlines for research in different scientific fields. Such a large facility costs rather great, and funding from government is a routine approach.

Industrial applications of synchrotron radiations attract great interests as well. And some compact light sources were built in a research institute for industrial users or in an industrial enterprise. Most industrial applications are in medicine, pharmacy, chemistry, mechanics, and food industry. Some new applications such as EUV lithography are under exploration.

INDUSTRIAL APPLICATIONS

Industrial application is a direct way for synchrotron radiation to benefit the society and improve people's life quality. With rapid growth of industrial demand, various applications of synchrotron radiation have been developed.

Medical Applications

High energy photos can be used in the medical industry in many aspects including physical examination, cancer treatment, pharmacy and so on. X-ray is one of the most common ways for health checkup, and it is also a main part in the spectrum of synchrotron radiation. Gamma ray, which can be radiated from a compact accelerator using techniques such as Compton backscattering, has been used to break the DNA inside cancer cells, stop cancer from growing and cause its death eventually.

In hospitals synchrotron radiations from compact accelerators can be used for medical treatment, while pharmacy industry can use high intensity synchrotron radiations to improve efficiency of medicine research and development. X-ray has been used for protein structure analysis, and new medicine can be developed more efficiently. Another application of X-ray in medicine industry is to reform the drug particles and to conduct a proper distribution of different components.

Chemical and Mechanical Industry

Catalyst plays an essential role in chemical industry, and synchrotron radiations can help to develop and manufacture high-efficiency kind. Other important applications of synchrotron radiation in chemical industry include material characteristics improvement etc. Using X-ray to detect flaws in solid object is a common approach for its merits such as flexibility, damage-free, and so on.

Radiation Sterilization

Sterilization can help to preserve food for a long time. Radiation can be used to sterilize the products of food industry in a rather quick and easy-to-tune manner. Compact accelerator is a good option to provide radiations the food industry needs.

EUV Lithography

Synchrotron radiation as a solution of light source for EUV lithography has been under exploration for years. Comparing to LPP (Laser-Produced Plasma) and DPP (Discharge Produced Plasma) light sources, compact accelerators can provide EUV light with high density and high collimation without pollution from metal particles or plasma ions.

* Work supported by the Youth Innovation Promotion Association of Chinese Academy of Sciences (No.2020287)

† Email address: zhangql@sari.ac.cn

GENERALIZED LONGITUDINAL STRONG FOCUSING: A RING-BASED BEAM MANIPULATION TECHNIQUE

Zizheng Li, Xiujie Deng, Zhilong Pan, Chuanxiang Tang*,

Tsinghua University in Beijing (TUB) Accelerator Laboratory Department of Engineering Physics

Alex Chao[†], SLAC National Accelerator Laboratory (SLAC)

Abstract

Generalized longitudinal strong focusing (GLSF), a ring-based beam manipulation technique, has been proposed to generate steady-state, nanometer-long electron bunches in laser-driven storage rings. Coherent EUV radiation can thus be produced with greatly enhanced power and photon flux, benefiting a wide range of scientific and industrial communities. The GLSF mechanism invokes precise transverse-longitudinal coupling dynamics and exploits the ultralow vertical beam emittance. In a GLSF ring, kW-level coherent EUV radiation is attainable.

INTRODUCTION

Storage rings have driven great progress in science and technology for being stable, reproducible, and clean photon sources. Alongside the pursuit of low transverse emittance in recent decades, beam manipulation methods in storage rings flourish as well in longitudinal dimension. Bunches as short as picoseconds can be produced when rings operate in the low- α mode [1, 2].

Ambition to further shorten ring-stored bunches continues. Laser-driven storage rings have been proposed where laser modulators are used for bunching instead of RF cavities [3–6]. With a modulation wavelength reduction of roughly six orders of magnitude, the equilibrium bunch length can be notably decreased to tens of nanometers or even less. The longitudinal weak focusing (LWF) scheme employs low- α and low-partial- α optics to control bunch lengthening from stochastic photon emission [7, 8]. In a longitudinal strong focusing (LSF) ring, multiple laser modulators are included as longitudinal focusing elements, or ‘longitudinal quadrupoles’ [9, 10]. Bunches are strongly manipulated in longitudinal dimension and tailored to be short at specific locations of the ring.

It is challenging, yet rewarding, to manipulate steady-state bunches of nanoscale length in storage rings. These bunches are ideal producers of coherent extreme ultraviolet (EUV) radiation with greatly enhanced average power and photon flux desired by a wide range of applications. The boosted EUV photon flux within a narrow bandwidth has been craved by high-energy-resolution angle-resolved photoemission spectroscopy [11, 12]. In sub-meV bandwidth, key electronic structures may be probed, and findings in condensed matter physics could be made. The high average power of coherent EUV radiation suggests that a storage ring-based light source is a promising option for EUV lithography [13, 14]. Output

power may be tripled from existing facilities, leading to a huge promotion in microchip production. In addition, the produced photon pulse trains with pulse duration of tens of attoseconds is longed for by attosecond physics studies [15]. Besides, once ignored features of beam dynamics may now come to light, opening up a thrilling new frontier for accelerator physics.

Obstacles, however, prevent existing methods from being fully competent when attempting to obtain steady-state nanometer-long bunches on a turn-by-turn basis. Reducing the bunch length in the LWF scheme to nanometers calls for momentum compaction that is presently too low to be technically feasible, while the power of the modulation laser required by the LSF scheme exceeds the capacity of current optical cavities in continuous-wave mode.

A ring-based beam manipulation technique is then desired where coherent EUV radiation could be generated turn by turn. The power of the modulation laser should be controlled below 1 MW, which optical cavities could bear for continuous-wave mode operation. Besides, the status of electron bunches should be recovered after compression. This is pivotal in storage rings, unlike in single-pass devices.

GENERALIZED LONGITUDINAL STRONG FOCUSING (GLSF)

In this paper, a ring-based beam manipulation technique, generalized longitudinal strong focusing (GLSF), is proposed to produce coherent EUV radiation turn by turn in laser-driven storage rings.

Strong manipulation is imposed and significant variation in bunch length is present in both LSF and GLSF schemes. The way electrons are handled, however, is different. Instead of manipulation in the longitudinal dimension alone, GLSF rings deliberately invoke transverse-longitudinal coupling beam dynamics. The GLSF scheme takes advantage of the extremely low vertical beam emittance in a horizontal-vertical-uncoupled planar ring, by projecting which a short bunch length can be attained with significantly reduced power of modulation lasers. Cancellation of the introduced coupling and modulation after the beam radiates is required to retain an uncoupled bunch and maintain the low vertical beam eigen-emittance, which is intended to be used again in following turns.

Calculation with practical beam parameters shows that kW-level quasi-continuous-wave coherent EUV radiation can be achieved turn by turn in a GLSF ring with a modulation laser power as low as 1 MW, allowing for continuous-wave operation of state-of-the-art optical cavities.

* tang.xuh@tsinghua.edu.cn

[†] achao@slac.stanford.edu

STUDY ON XiPAF SYNCHROTRON NONLINEAR DYNAMICS*

X. Y. Liu^{1,2,3}, H. J. Yao^{1,2,3†}, Y. Li^{1,2,3}, Z. J. Wang^{1,2,3}, Y. Xiong^{1,2,3}, P. Z. Fang^{1,2,3}
S. X. Zheng^{1,2,3}, X. W. Wang^{1,2,3}, Z. M. Wang⁴

¹Key Laboratory of Particle & Radiation Imaging, Tsinghua University, Beijing, China

²Laboratory for Advanced Radiation Sources and Application, Tsinghua University, Beijing, China

³Department of Engineering Physics, Tsinghua University, Beijing, China

⁴State Key Laboratory of Intense Pulsed Radiation Simulation and Effect
(Northwest Institute of Nuclear Technology), Xi'an, China

Abstract

Xi'an Proton Application Facility (XiPAF) has been operational since 2020, which can accumulate 2×10^{11} protons after injection and 1×10^{11} protons after acceleration. In this paper, we have investigated the XiPAF synchrotron nonlinearity by simulation and experiments. The beam loss occurs with the resonance $\nu_x + 2\nu_y = 5$ in the absence of space charge, and the resonance $2\nu_x - 2\nu_y = 0$ in the presence of space charge. The stripping foil also plays an important role due to its multiple scattering effect and ionization energy loss effect.

INTRODUCTION

The Xi'an Proton Application Facility (XiPAF) is the first facility that is dedicated to simulations of the space radiation environment in China [1], which consists of a 7 MeV linac injector and a compact 200 MeV synchrotron. After several rounds of machine studies and experiments from 2020, the XiPAF synchrotron can accumulate 2×10^{11} protons after injection and 1×10^{11} protons after acceleration [2, 3].

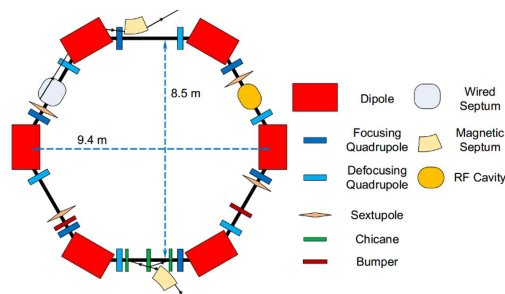


Figure 1: XiPAF synchrotron lattice layout.

The XiPAF synchrotron has 6 periods, with a “missing dipole” lattice structure, shown as Fig. 1. The circumference is 30.9 m, stripping injection turns negative hydrogen beam to proton beam, then the RF cavity voltage ramps from 60 V to 600 V within 10 ms adiabatically, and accelerates particles to 200 MeV. The main parameters are shown in Table 1, and the lattice beta functions are shown as Fig. 2.

During beam commissioning, we found that nonlinear resonance is the main limitation during injection, capture and acceleration. In this paper, the nonlinear dynamics of

Table 1: XiPAF Synchrotron Main Parameters

Parameters	Values	Units
Periodicity	6	
Circumference	30.9	m
Injection Energy	7	MeV
Injection Tune ν_x/ν_y	1.74 / 1.70	
Extraction Energy	10~200	MeV
Extraction Tune ν_x/ν_y	1.68 / 1.72	
Natural Chromaticity	-0.32 / -2.39	
Momentum Compaction	0.34	

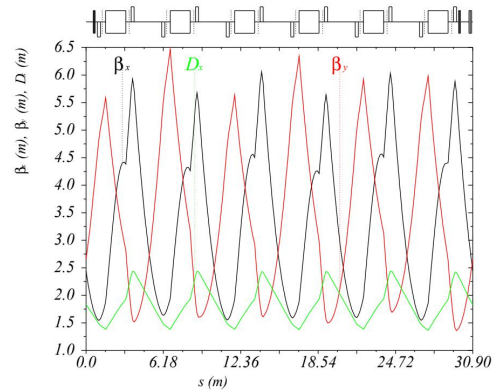


Figure 2: XiPAF synchrotron lattice optics.

the XiPAF synchrotron have been studied, with and without space charge. Possible resonance has been analysed in tune diagram, resonance stopband scan has been used to identify the nonlinearity of the XiPAF synchrotron by simulation and experiment, and the space charge effect has also been discussed.

RESONANCE LINE AND HARMONIC ANALYSIS

The XiPAF synchrotron has 6 periods. Lattice optics functions are shown as Fig. 2, beta function is not fully symmetric according to the 3 chicane magnets located in the injection long drift section, which are used for stripping injection. Harmonic analysis of beta function shows that the strongest harmonic number is 6 (as shown in Fig. 3), which is the same with the lattice period. Because of the symmetry distortion of chicane magnets, the strength of all harmonic

* Work supported by National Natural Science Foundation of China (No. 12075131)

† yaohongjuan@tsinghua.edu.cn

EVALUATION OF FIELD QUALITY FOR ELLIPTICAL AND CURVED MAGNETS

Jie Li, Kedong Wang*, Xueqing Yan, Kun Zhu†,

State Key Laboratory of Nuclear Physics and Technology, and Key Laboratory of HEDP of the Ministry of Education, CAPT, Peking University, Beijing, 100871, China

Abstract

The elliptical magnetic field zone is a useful tool for beam distribution homogenization and FFAG accelerators. Additionally, strongly curved magnets are studied for their application in beam transmission and nuclear fusion. However, traditional magnetic measurements, known as field harmonics, for straight magnets are not suitable for these two kinds of special magnets. In this article, advanced multipoles are used to characterize the fields of straight magnets with elliptical apertures and 2D axisymmetric enclosed curved magnets. The article provides a detailed analysis of magnetic fields using data from FEA or Biot-Savart law. Furthermore, the article discusses methods for characterizing the field quality of unclosed curved magnets used for gantry.

INTRODUCTION

Magnets are crucial components for beam transport, and their configuration depends on the specific usage scenario. In this article, we will focus on the evaluation of field quality in strongly curved and elliptical magnets. By utilizing advanced multipoles, we can determine the field in the central part based on the field data from reference curves [1].

CURVED MAGNETS

When evaluating the central magnetic field of an accelerator magnet, it is common to expand it in terms of circular multipoles, such as dipole, quadrupole and sextupole flux density distributions. The multipole coefficients, also known as field harmonics, are obtained using the Fourier series expansion of the magnetic field component along a circle. These coefficients can also represent the Taylor coefficients of a series expansion of the flux density at the horizontal or vertical axis. They are the transverse coordinates in the co-moving beam coordinate system. However, this approach is not suitable for strongly curved magnets. When particles traverse a curved orbit, they experience a magnetic field up to second order as follows.

$$\begin{aligned} \frac{ec}{\beta E} B_x &= -\kappa_y - kx + ky - \frac{1}{2}m(x^2 - y^2) \\ &+ mxy + \frac{1}{2}(-\kappa_y k + \kappa_x k + \kappa_y'')x^2 \\ \frac{ec}{\beta E} B_y &= +\kappa_x + ky + kx + \frac{1}{2}m(x^2 - y^2) \\ &+ mxy - \frac{1}{2}(\kappa_x k + \kappa_y k + \kappa_x'')y^2 \end{aligned}$$

* wangkd@pku.edu.cn

† zhukun@pku.edu.cn

It is clear that different orders are mixed in the magnetic field if curvature is not zero. The Fourier coefficients from the reference circle deviate from the Taylor coefficients at the transverse coordinate axis. In beam dynamics, we are interested in the latter one. Assuming axial symmetry for a curved magnet, solutions of the vector Laplace equation can be found using bipolar coordinates in Fig. 1, where $k = \cosh \eta - \cos \xi$. Here are the expressions for the azimuthal magnetic vector potential inside and outside the current shell.

$$A_\phi^{in} = k^{1/2} [-b_n \cos(n\xi) + a_n \sin(n\xi)] Q_{n-1/2}^1(\cosh \eta) \quad (1)$$

$$A_\phi^{out} = k^{1/2} [-d_n \cos(n\xi) + c_n \sin(n\xi)] P_{n-1/2}^1(\cosh \eta) \quad (2)$$

One advantage of using bipolar coordinates is that the iso- η lines are circular, although their centres may differ slightly from the focuses. Typically, we require the good field region to be circular. Our goal is to reconstruct the magnetic field based on point data acquired along a reference circle.

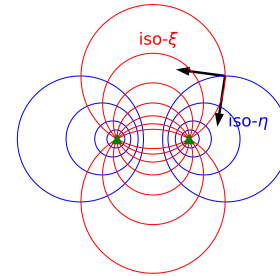


Figure 1: Bipolar coordinates.

The corresponding patterns of magnetic field, including normal and skew patterns, are shown in Fig. 2. It should be noted that the normal $n = 0$ pattern does exist. Associated Legendre functions with half-integer indexes are used, we can calculate the value from this paper [2]. With the increase of the value that bend radius divided by the bore radius, the focus approaches the bore centre, and traditional multipoles recover. Here are the expression of the magnetic field inside the current shell.

$$\begin{cases} B_\xi^{in} = \frac{-b_n k^{3/2}}{a} \left[\frac{n+\frac{1}{2}}{\tanh \eta} Q_{n-1/2}^1 - \frac{1}{2} \sinh \eta k^{-1} Q_{n-1/2}^1 \right. \\ \quad \left. - \frac{n+\frac{1}{2}}{\sinh \eta} Q_{n-3/2}^1 \right] (-\cos n\xi) \\ B_\xi^{in} = \frac{-a_n k^{3/2}}{a} \left[\frac{n+\frac{1}{2}}{\tanh \eta} Q_{n-1/2}^1 - \frac{1}{2} \sinh \eta k^{-1} Q_{n-1/2}^1 \right. \\ \quad \left. - \frac{n+\frac{1}{2}}{\sinh \eta} Q_{n-3/2}^1 \right] \sin n\xi \end{cases}$$

$$\begin{cases} B_\eta^{in} = \frac{-b_n k^{3/2}}{a} \left[-n \sin n\xi - \frac{1}{2} k^{-1} \sin \xi \cos n\xi \right] Q_{n-1/2}^1(\cosh \eta) \\ B_\eta^{in} = \frac{-a_n k^{3/2}}{a} \left[-n \cos n\xi + \frac{1}{2} k^{-1} \sin \xi \sin n\xi \right] Q_{n-1/2}^1(\cosh \eta) \end{cases}$$

If we obtain magnetic field data at several points sampled along a reference circle, the Fourier coefficients of the radial field B_ρ directly represent the multipole strength for straight

GENERAL DESIGN OF 180 MHz RFQ FOR BNCT

Zhi-Qiang Ren, Xin-Miao Wan, Yu-Fei Yang, Peng-Tai Lin, Wen-Long Liao, Xiao-Bao Luo, Xue-Jiang Pu, Zhi-Hui Li†

The Key Laboratory of Radiation Physics and Technology of Ministry of Education, Institute of Nuclear Science and Technology, Sichuan University, Chengdu 610065, China

Abstract

Accelerator based boron neutron capture therapy (AB-BNCT) is a promising cancer treatment technology. A general design has been proposed of a 180 MHz radio frequency quadrupole (RFQ) accelerator for BNCT. The particularity of dynamic design of the RFQ is that the average aperture radius changes along the accelerator. Beam dynamics design results show that the length of accelerator which accelerates protons from 35 keV to 2.81 MeV is 5.07 m, and the transmission up to 99.65%. Meanwhile, 20 pairs of Pi-mode stabilizer rods are considered to keep the frequency of dipole mode away from the working quadrupole mode. The simulation results show that a large mode separation of more than 20 MHz between the operating quadrupole mode and nearest dipole mode can be obtained, this is sufficient to deal with the errors caused by machining and misalignment. The initial insertion depth

BEAM DYNAMICS DESIGN

BNCT requires sufficient flux (10^9 n/cm²/s) of epithermal neutrons (0.5 eV ~ 10 keV), because of this, an RFQ accelerator has been proposed: accelerating 25 mA proton beam (continuous wave mode) to 2.8 MeV to meet the requirements of BNCT. Based on the requirement of high beam transmission efficiency (greater than 99%), the beam dynamic design adopts the idea of making the average aperture variable along the accelerator 0. The beam dynamic parameters are shown in Figure 1.

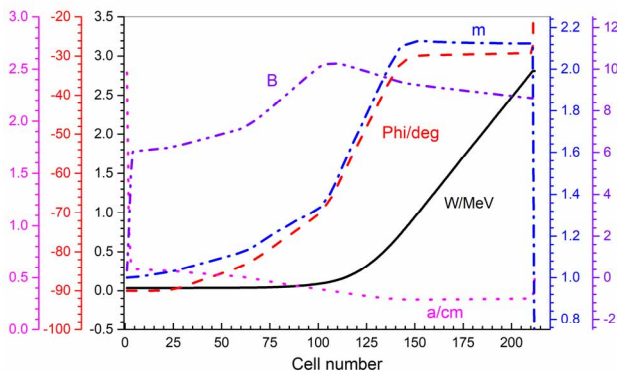


Figure 1: RFQ Accelerator beam dynamic parameters.

As for beam dynamic simulations, 10^5 macro particles with an initial 4D water-bag distribution are simulated with PARMTEQM 0, as shown in Figure 2 and Figure 3.

* Work supported by the National Natural Science Foundation of China (Grant Nos. 11375122 and 11875197)
† lizhahui@scu.edu.cn

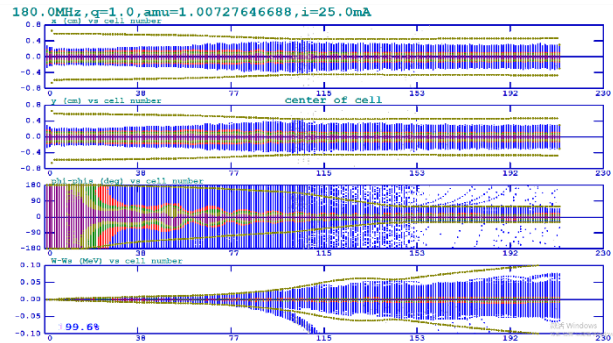


Figure 2: RFQ beam transmission process of the RFQ.

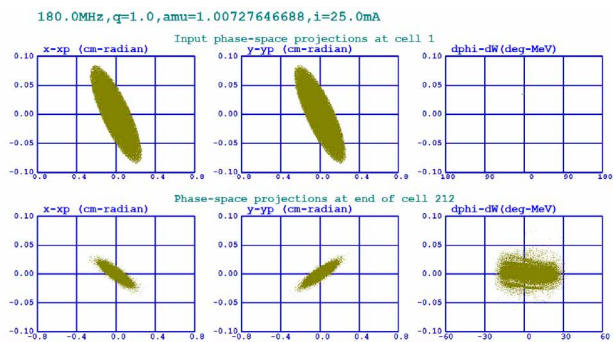


Figure 3: Beam profiles at the entrance and exit of the RFQ.

After simulation, the parameter results are shown in Table 1.

Table 1: Simulation Results

Parameter	Value
Frequency	180 MHz
Input energy	35 keV
Output energy	2.81 MeV
Voltage	72 kV
Current	25 mA
ϵ_t (norm. rms, entrance)	0.20π .mm.mrad
ϵ_t (norm. rms, exit)	0.22π .mm.mrad
ϵ_l (norm. rms, exit)	0.62π .mm.mrad
Vane length	507.73 cm
Transmission	99.65 %

CROSS SECTION DESIGN

The design and simulation of a full length 3D model of whole cavity is usually based on slice cavity. By simulation with slice cavity, some high frequency parameters of the cavity can be obtained easily and the approximate range of cavity size L (shown in Figure 4) can be quickly

DYNAMICS DESIGN ON 70-250MeV PROTON LINAC*

Yu-Fei Yang, Xin-Miao Wan, Zhi-Qiang Ren, Peng-Tai Lin, Zhi-Hui Li†

The Key Laboratory of Radiation Physics and Technology of Ministry of Education, Institute of Nuclear Science and Technology, Sichuan University, Chengdu 610065, China.

Abstract

Charged proton beams have broad application prospects, and research on compact S-band proton linear accelerators is increasingly heating up in recent years. For radiation therapy, to achieve the conventional penetration range of water-equivalent tissues, protons with energy of 70 to 230 MeV are required. The design of electromagnetic structure is closely related to particle dynamics design. A flexible and controllable particle dynamic tracking code (PDT) through both traveling wave and standing wave acceleration has been compiled to simulate particle trajectory and satisfy automatic tuning of the various components in the entire acceleration chain. The linac with a total length of approximately 7.89 m composed of 16 tanks of backward traveling wave structures and permanent magnet quadrupole lenses was designed, operating at an RF frequency of 2.856 GHz with a target acceleration gradient of 30 MV/m, and accelerating proton beam from 70 MeV to 250 MeV while maintaining low emittance and high transmission efficiency.

INTRODUCTION

Proton linear accelerator is widely used in basic research, medical treatment, and industrial manufacturing, among other fields. It can be used in the manufacture of microelectronic devices, surface modification of materials. Currently, it's mainly concentrated in the field of radiation therapy. Compared with advanced photon therapy technologies such as intensity-modulated radiation therapy and volumetric arc therapy, proton therapy can significantly reduce the dose of radiation to normal tissue surrounding the tumor, reducing the possibility of inducing second primary tumors [1]. Traditional proton therapy equipment is bulky, difficult to install and manufacture, and expensive, making it difficult to be widely promoted. Currently, research into miniaturization and compactness of proton linear accelerator is underway worldwide.

Currently, the main high-gradient RF acceleration structures include the TeV Energy Superconducting Linear Accelerator (TESLA) structure [2], Coupled Cavity Linac (CCL) [3], and Backward Traveling Waveguide (BTW) structure [4] is used in the TULIP project, which is dedicated to developing a compact proton linac capable of achieving an accelerating gradient of 50 MV/m, and peak surface electric field and shunt impedance within acceptable ranges even in low- β configurations. Due to the scarcity of simulation software for proton acceleration using traveling wave architecture, we utilized our own

compiled open-source particle dynamic tracking code (PDT) based on traveling wave acceleration to conduct preliminary dynamic design of a 70-250 MeV BTW proton linac.

PDT CODE

Compared with the abundant available design tools for standing wave proton linac, the design tool for tracking protons through traveling wave structures is relatively hard to find. Most particle tracking programs are designed to handle standing waves or use the superposition of two standing waves to approximate traveling waves, making them unsuitable for BTW structures. Additionally, these programs often function as closed systems, limiting customize and expand the solver capabilities according to our specific requirements.

Due to the unique demands of proton therapy, it is necessary to adjust the kinetic energy of the output particles within a certain range while maximizing the transmission efficiency. This implies that the PDT code not only needs to simulate the particles trajectories through acceleration channel but also incorporate the beam matching functionality [5]. *TraceWin* is capable of calculating the transfer matrix of a given structure and handling standing wave electromagnetic field map represented by real numbers, whereas PDT code accepts not only real numbers but also traveling wave with complex numbers. Since the electromagnetic structure design and particle dynamics design are closely related, it is important to find a starting point.

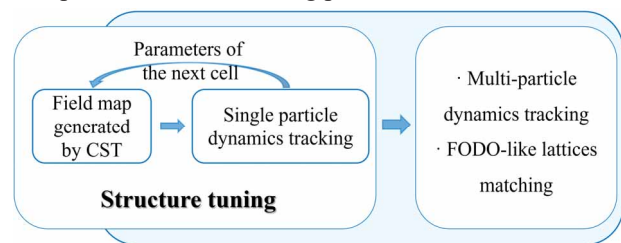


Figure 1: The Simplified scheme of PDT code architecture.

The commonly used simulation software CST studio suite [6] makes it feasible to extend the use of the program to traveling wave structures. CST is used to model and tune the single cell for calculating the electromagnetic field map, while MATLAB serves as the core of the code. The whole solving process is mainly divided into two modules. Since the RF structure design and particle dynamics design are closely related, it is important to find a starting point. In the first part, it makes full use of automated MATLAB and CST co-simulation to track the dynamics of a single particle in the longitudinal direction and tune waveguide structure as an interactive multi-run simulation. has added

* Work supported by the National Natural Science Foundation of China (Grant Nos. 11375122 and 11875197)

† lizhihui@scu.edu.cn

CONTROL OF CAFE BEAM ENERGY USING LINEAR ACCELERATOR SIMULATION SOFTWARE AVAS AND BEAM LINE CALIBRATION TECHNOLOGY*

Chao Jin, Chi Feng, Xin Qi[†], Zhijun Wang, Yuan He[†], Institute of Modern Physics, Lanzhou, China
 also at Advanced Energy Science and Technology Guangdong Laboratory, Huizhou, China

Abstract

A new accelerator simulation code named Advanced Virtual Accelerator Software (AVAS) was developed by the Institute of Modern Physics, Chinese Academy of Science. Although the code is proposed to simulate the particle transport in the linac of the China Initiative Accelerator Driven System (CiADS), it can be also used for common linacs. We have constructed a framework for the accelerator simulation program AVAS based on the structure, function, parameters, errors, and operational logic of real accelerators. The mapping relationship between the operating parameters and simulation parameters of the Chinese ADS Front-end Demo Linac (CAFe) superconducting section was successfully established through AVAS. In the testing experiment, AVAS successfully set the operating parameters of the CAFe superconducting section, and the deviation between the energy setting value and the actual measurement value was about 0.5%.

INTRODUCTION

AVAS [1] is a linear accelerator simulation code developed for the requirements of the CiADS [2]. The code is based on particle-in-cell (PIC) algorithm [3] and implemented in the C++ language. All accelerator elements as well as algorithms are packaged into an executable program, which can be run after installation on the windows operating system. On the one hand, AVAS has developed the S-PICNIC [4] algorithm by improving the standard PICNIC [5] algorithm, which significantly reduces the computational effort to solve for space charge effects. On the other hand, AVAS achieves efficient parallelism. The above work has resulted in a significant reduction in the AVAS multi-particle simulation time, which is a significant advantage in large-scale multi-particle simulations.

The operating parameters of the accelerator are different from those used in the accelerator simulation program. In order to obtain the operating parameters of the accelerator directly from the numerical simulations, it is necessary to establish a correspondence between the operating parameters of the accelerator and the numerical simulation parameters. In this paper, AVAS program is introduced first, and then how to establish the corresponding relationship between accelerator operating parameters and AVAS simulation parameters is explained. Finally, it is tested on CAFe [6] superconducting section.

* Work supported by National Natural Science Foundation of China (Grant No. 11775282)

[†] email address: qxin2002@impcas.ac.cn, hey@impcas.ac.cn

MATERIALS AND METHODS

The CAFe is the pre-validation device for CiADS and is structured as shown in Fig. 1. In CAFe, the beam is mainly accelerated in the RF superconducting cavity and the energy of the exiting beam is determined by the parameters of the RF superconducting section. In this paper, we use AVAS to map the superconducting section of CAFe to achieve a process that gives the accelerator operating parameters directly through simulations and changes the beam energy.

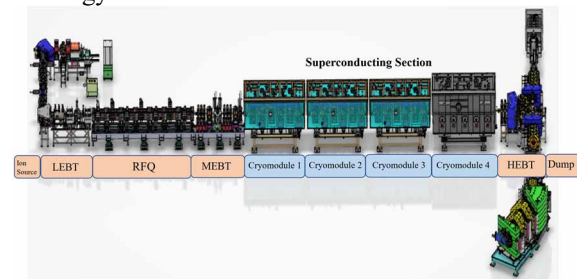


Figure 1: CAFe structure schematic.

The superconducting section of CAFe contains four cryomodules (Cryomodules 1-4), the exact composition of which is shown in Fig. 2. The first three cryomodules contain six solenoids and six RF cavities each, and the last cryomodule contains five solenoids and five RF cavities. The operating parameters of the solenoids are the current of the solenoid magnets and the operating parameters of the RF cavities contain the RF field amplitude and the RF field phase. Therefore, the superconducting section of CAFe has a total of 69 operating parameters. If these 69 operating parameters can be given directly by simulation when the beam energy needs to be changed, stable beam transmission can be achieved quickly.

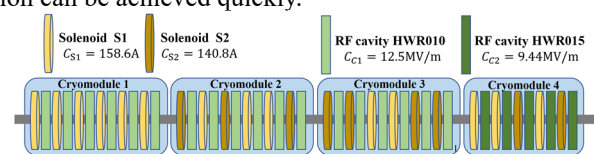


Figure 2: Cryomodule composition diagram.

These three types of parameters contain two types of mapping relationships, one for magnitude, including solenoid current and RF field amplitude, both of which are linearly related to the magnitude of the electromagnetic field (EMF) in the corresponding element, which is controlled in AVAS by adjusting the magnification of the reference electromagnetic field. Therefore, it is necessary to determine the proportionality constants between the reference EMF and the real EMF per unit current (or per unit RF field

MULTIPOLE FIELD OPTIMIZATION OF X-BAND HIGH GRADIENT STRUCTURE

B. Feng[†], Q. Gao^{*}, J. Shi, H. Zha, X. Lin, H. Chen, Department of Engineering Physics
Tsinghua University, Beijing, China

Abstract

The X-band constant gradient acceleration structure plays a crucial role in the VIGAS project. However, the presence of a multipole field component in the structure's coupler leads to an increase in ray bandwidth and a decrease in yield, ultimately affecting the quality of the generated rays. Through calculations, it has been determined that the quadrupole field component is particularly prominent in the original structure, accounting for 29.5% of the fundamental mode strength. Therefore, it is necessary to modify the cavity structure of the coupler. By altering the shape of the cavity to two staggered circles, the objective of reducing the quadrupole field is achieved. The optimized quadrupole field component now accounts for approximately 0.3% of the fundamental mode strength. Subsequently, the non-resonant perturbation method was employed to simulate and experimentally measure the magnitude of the multipole field component in the actual acceleration cavity.

INTRODUCTION

In 2021, Tsinghua University introduced the Very Compact ICS Gamma-ray Source project, known as the VIGAS project. The primary objective of the VIGAS project is to develop the world's first compact quasi-monochromatic gamma-ray source operating in the megaelectronvolt range. The gamma-ray energy generated by this project can be continuously adjusted within the range of 0.2 to 4 MeV.

The accelerator structure utilized in the project is based on the X-band technology and comprises an input coupler and an output coupler positioned at its ends. However, the inclusion of these couplers disrupts the circular symmetry of the accelerator structure, resulting in the emergence of multipole fields within the electromagnetic field. These multipole fields, present within the accelerator structure, have the potential to increase the beam emittance. Consequently, this may have an impact on the beam dynamics, ultimately affecting the bandwidth and yield of the produced gamma rays [1].

To analyze the beam dynamics, comprehensive simulations were conducted for the entire accelerator structure. These simulations took into account three-dimensional field distributions for the various components, specifically focusing on comparing the effects of one-dimensional and three-dimensional field distributions within the X-band accelerator structure. The results demonstrate that the emittance, which characterizes the size of the beam, increases by approximately 14% in the presence of three-dimensional field distributions, compared to the case of one-

dimensional field distributions. This indicates that the presence of multipole fields indeed leads to an increase in the emittance.

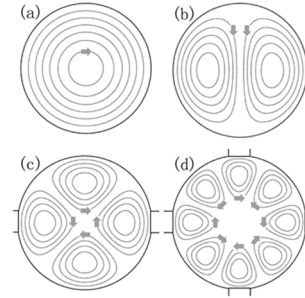


Figure 1: Different drilling situation in the cavity and the distribution of the multi-pole magnetic field.

The emergence of multipole fields within the couplers is a result of the symmetry breaking of the cavity, as shown in Fig. 1 [2]. In the absence of any deviations from perfect circular symmetry, the occurrence of multipole fields can be avoided. However, the introduction of a hole in the cavity wall gives rise to the generation of multipole fields, with the dipole field being the most dominant component. In the case of a pair of symmetric double holes, the quadrupole field becomes the strongest component of the multipole fields. When there are four symmetric holes, the octupole field emerges as the most significant component.

In the existing X-band accelerator structure's couplers, two symmetric holes are present, resulting in the quadrupole field being the most prominent among the multipole fields. It constitutes approximately 30% of the intensity of the fundamental mode. Hence, it becomes crucial to suppress the quadrupole field component effectively.

OPTIMIZATION

The most effective method to suppress the quadrupole field component is by introducing two additional holes in the vertical direction of the previously symmetrical double holes, forming a symmetric four-hole structure. This modification effectively mitigates the quadrupole field. However, the process of punching additional holes has a considerable impact on the structure. Therefore, a compromise approach was adopted. The entire cavity of the coupler was transformed from a circular structure to two staggered circular structures, creating a racetrack-type structure, as shown in Fig. 2. This approach provides a satisfactory solution to reduce the quadrupole field.

[†] fby22@mails.tsinghua.edu.cn

^{*} gaoq08thu@tsinghua.edu.cn

DESIGN OF A LARGE MOMENTUM ACCEPTANCE GANTRY BASED ON AG-CCT FOR LIGHTWEIGHT PROTON THERAPY FACILITY*

Yicheng Liao, Wei Wang, Xu Liu, Ruiying Luo, Bin Qin[†]
State Key Laboratory of Advanced Electromagnetic Technology,
Huazhong University of Science and Technology, Wuhan, China

Abstract

Superconducting (SC) gantry can be applied to proton therapy with significantly reduced footprint and weight. However, the relatively lower ramping limit of the SC magnetic field becomes a bottle-neck for fast energy change and beam delivery. Designing a large momentum acceptance (LMA) beam optics can mitigate this issue, which would, meanwhile, bring potential applications for advanced treatment schemes with high beam transmission. In this contribution, we present the design of an LMA gantry using strong focusing AG-CCT SC magnets and symmetrical achromatic lattice. A fast degrader is combined in this design so that the gantry can perform rapid energy switches during the treatment. The AG-CCT design process and beam transport simulation are all performed with our homemade integrated code CSPT, which has interfaces to Geant-4 and Opera, and can reach a maximum speed-up ratio of 450 by applying parallel computation technique. The multi-particle tracking result proves that the gantry has a large momentum acceptance of ~20%.

INTRODUCTION

Hadron therapy is known to have superior physical characteristics, namely Bragg-Peak. It decreases the deposit dose to surrounded normal tissues and thus holds the potential of reducing the toxicity of organs at risk. Gantry, as an attractive tool in particle therapy, can further expand the ability of conformal treatment by irradiating the beam from different angles. However, the relatively large magnet rigidity, with respect to that of electrons in photon therapy, leads to massive facility size and weight. Most of the gantries running for proton therapy weigh over 100 tons with their length exceeding 10 m [1]. The figure would be much larger when it comes to carbon-ion facilities. Therefore, a cost-effective hadron therapy facility with a smaller gantry is one of the major interests of hospitals and research centers.

Utilizing superconducting (SC) technology enables the magnet to excite a higher magnetic field, which, in consequence, can make the gantry significantly lighter. The main drawback of the SC magnets is their slow ramping rate. The momentum modulation process in the steps of $\Delta p/p = 1\% \sim 2\%$ is performed with a ramping time of 0.1 ~ 2.0 s per step, corresponding to the momentum of the beam [2]. Designing a gantry lattice with large momentum acceptance (LMA) can mitigate this issue so that the field of

magnets maintains while the beam with various momentum can still be transported to the iso-center. This contribution presents the design of an LMA gantry for proton therapy using alternating gradient canted cosine theta (AG-CCT) magnets. The beam lattice with a fast degrader component and a compact nozzle design is introduced in the paper. For the convenience of the gantry design, a simulation toolkit based on parallel computation technology is developed. A preliminary design of the AG-CCT magnet is displayed at the end.

OPTICS DESIGN OF THE LMA GANTRY

The overview of the LMA gantry is presented in Fig. 1, which is a cyclotron-based design. A fast degrader component is placed in the middle of the gantry for momentum modulation. The degrader adopts a pair of high-density graphite wedge for continuous momentum modulation, and 2 B_4C blocks for step modulation, since the low Z material can suppress the growth of beam emittance. Linear motors could be equipped for fast energy switches. Two copper collimators lie in sequence, right after the degrader, for emittance restriction. At this stage, only one set of collimator configuration is applied to form a beam with the emittance of 10π mm mrad for the following beamline. The Monte Carlo (MC) simulation suggests that the overall transmission efficiency at the nominal energy 70 MeV is about 0.91%, which is about 53% higher than the traditional multi-wedges degrader.

On either side of the degrader component are the 2 bending sections, among which only the second bending section is demanded to have a large momentum acceptance of >16% to ensure a sufficient range of momentum variation with a fixed field of the SC magnet. Considering such a large momentum offset, high-order aberration should be taken into account. AG-CCT is introduced in the design as a main achromatic method [3], and its magnetic field is symmetrically arranged. Due to its flexibility of combining the dipole with multipole fields, the quantity of the magnet in the gantry is reduced. A strong alternating quadrupole field is embedded in the magnet for restricting the beam of different nominal momentum within the bore. Weak sextupole is added for high-order achromaticity. The optics design and optimization process is carried out on COSY Infinity [4]. The optics result of the second bending section is presented in Fig. 2, a stable rounded beam spot is formed at the iso-center, which proves that the gantry is capable of delivering the beam with a momentum range of -9.5%~+10.5%. The main restriction of the momentum acceptance is the good

* Work supported by the National Natural Science Foundation of China under Grant 11975107, 12205111.

[†] bin.qin@mail.hust.edu.cn

RESEARCH ON FIRST HARMONIC SHIMMING METHOD OF CYCLOTRON BASED ON LEAST NORM SQUARE SOLUTION

J. Lu[†], S. An, T. Bian, China Institute of Atomic Energy, Beijing 102413, China

Abstract

The magnetic field measurement of cyclotron and the shimming of isochronous magnetic field are one of the important links in cyclotron. Due to the influence of factors such as processing errors, installation errors, and inhomogeneity of the magnetic properties of magnet materials, the main magnetic field of the cyclotron will usually deviate from the required isochronous magnetic field and contain a certain amplitude of the first harmonic magnetic field. The existence of the first harmonic magnetic field will rapidly increase the transverse oscillation amplitude and cyclic emittance of the particles, eventually causing beam loss. In order to improve the beam quality of the cyclotron, the shimming technology of the first harmonic magnetic field is essential. In this paper, through the finite element simulation calculation of the main magnet of the cyclotron, a quantitative algorithm for the first harmonic shimming based on the least norm square solution is proposed. At present, this method is being prepared for apply to the magnetic field shimming of the 10MeV high-current proton cyclotron of the CIAE.

Introduction

Due to the influence of internal defects of iron materials, machining errors and other factors, the magnetic field of the cyclotron usually contains the first harmonic component. During a particle moves in a non-ideal magnetic field, it will be subjected to an additional external force. The lateral oscillation of the particle caused by the external force is a forced oscillation, which will increase the amplitude of the lateral oscillation. When certain conditions are met, it will also cause resonance and cause the particle loss. When constructing a cyclotron, the first harmonic component of the magnetic field must be eliminated, so as to avoid the influence of forced oscillation on the lateral motion of particles and improve the quality of the beam.

The traditional first harmonic shim method is based on the Hard-edge mode method. The hard-edge approximation can be used on transforming the field error to the shape change. However, the accuracy of the calculation results is relatively low. Since a conservative strategy with scaling factor should be adopted to avoid over-shimming and oscillations [1]. For high-current cyclotrons, in order to achieve the physical goal of high-current, the first harmonic component of the magnetic field must be precisely eliminated [2].

In this paper, a magnetic field shimming algorithm based on a multiple linear regression model is proposed to achieve quantitative and accurate shimming of the first harmonic component of the magnetic field.

* Work supported by CIAE

[†] email address: 359037465@qq.com.

Principle of Shimming Algorithm

The research on the shimming algorithm and calculation method proposed in this paper is carried out on the basis of the simulation calculation of the compact cyclotron model shown in Fig. 1, through the software Opera-3d. Compared with the magnetic field distribution calculated by the TOSCA solver in the software and the actual measured magnetic field distribution, the error is within $\pm 0.5\%$ [3].

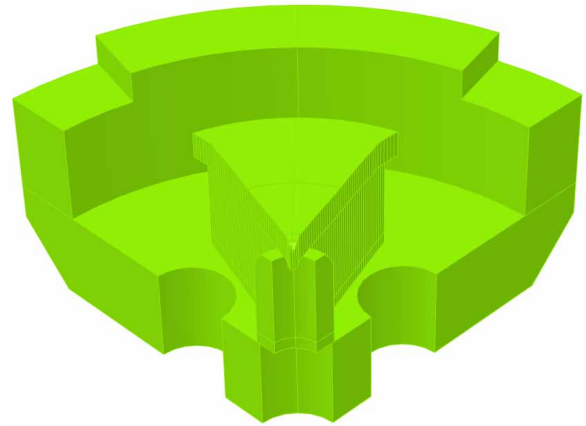


Figure 1: 10MeV cyclotron 1/4 model of CIAE.

The first harmonic magnetic field component of the compact cyclotron can be calculated by Fourier analysis, and the amplitude and phase of the first harmonic along the radial direction can be obtained by Eq. (1):

$$B(r, \theta) = B_0(r, \theta) + \sum_0^{\infty} b_{rk} \cos(k\theta + \beta_{rk}) \quad (1)$$

where $B_0(r, \theta)$ is the perfect magnetic field, b_{rk} is the harmonic amplitude, k is the harmonic coefficient, β_{rk} is the initial phase. The principle of shimming the first harmonic is: without changing the average magnetic field of the cyclotron, artificially introduce a reverse first harmonic to offset the first harmonic component of the original magnetic field. As shown in Fig. 2, in order not to change the average magnetic field, cutting at one pole must be supplemented at the other pole, but in the actual shimming process, the magnetic pole shimming can only be done by cutting. Fortunately, compared to the isochronous error of the magnetic field, the first harmonic magnetic field is a small amount, so the shimming of the first harmonic magnetic field can be included in the shimming process of the isochronous magnetic field, so as to solve the problem of the first harmonic shimming.

HIGH-FIDELITY MODELING AND TRANSMISSION OPTIMIZATION FOR THE BEAMLINE OF HUST-PTF *

Yu Chen, Bin Qin[†], Xu Liu, Wei Wang, Chengyong Liu

State Key Laboratory of Advanced Electromagnetic Engineering and Technology,
Huazhong University of Science and Technology, Wuhan, China

Abstract

A superconducting cyclotron-based proton therapy facility is under construction at Huazhong University of Science and Technology (HUST-PTF). In previous works, the vacuum chamber's shape and the tail effect of the energy spectrum are not considered when calculating the transmission efficiency of the beamline. This study proposes a high-fidelity modeling and optimization method for the HUST-PTF beamline based on Monte Carlo simulation using BDSIM. The modeling procedure of the beamline based on BDSIM is briefly introduced. Then verification of the optical parameters are performed on the gantry sections, and the transmission efficiency of the gantry is optimized by analyzing the unexpected beam loss. After optimization, the transmission efficiency at each energy setting point is calculated. The simulation results show that (1) the proposed optimization method improves the gantry's transmission efficiency from 92.4% to 95.6%; (2) the transmission efficiency calculated by high-fidelity modeling is more accurate than previous simulations because the beam-matter interaction and practical vacuum chamber geometry are considered.

INTRODUCTION

Huazhong University of Science and Technology is building a superconducting cyclotron-based proton therapy facility, and all magnet designs and installations have now been completed. Previous works have focused on the beamline's design [1], but evaluating the beamline's working state still using separated codes used in the design process may be unsuitable. The more realistic conditions should be considered. For beam tuning, it is of engineering significance to build a high-fidelity model to evaluate the operating state of the beamline and as a surrogate model.

The Refs. [2, 3] use beam delivery simulation software (BDSIM) to conduct seamless simulation on proton therapy systems for radiation protection. Their works consider the beam-matter interaction and practical vacuum chamber geometry. Inspired by their works, this study proposes a high-fidelity modeling and transmission optimization method with the HUST-PTF Beamline as a case study.

The remainder of this study is organized as follows: the model setup and the methodology are briefly introduced in Section II; the results are presented in Section III; and Section VI provides the study's conclusion.

* Work supported by the National Natural Science Foundation of China (11975107), and the National Key Research and Development Program of China (No. 2016YFC0105305).

[†] bin.qin@hust.edu.cn

THE MODEL SETUP AND METHODOLOGY

The HUST-PTF beamline is built and validated using BDSIM, a Geant4-based Monte Carlo program that simulates the dynamic motion of beam transport considering the particle-matter interaction and the vacuum chamber geometry [4]. As shown in Fig. 1, the HUST-PTF beamline includes three sections: (i). The energy selection section (ESS) modulates the beam energy and quality. (ii). The periodic transport section transmits the particles to each coupling point efficiently. (iii). The gantry section is to achieve multi-angle treatment. In addition, the physics list "g4qbbc", which includes pure hadronic parts consisting of elastic, inelastic, and capture processes, is used to simulate the physical process during the treatment.

The primary idea behind optimizing transmission efficiency is to analyze the beam loss process and use the gained insights to guide the constraints of the Transport code [5]. This approach achieves the desired results without resorting to complex algorithms. In the next section, this study will present a detailed account of how this study optimized the transmission efficiency of the gantry in the HUST-PTF beamline using this method.

THE RESULTS

To illustrate the consistency of the high-fidelity model constructed by BDSIM with the present design, the optical parameters need to be verified. Because the optical design does not include the energy modulation process, the beamline is divided into three segments for optical parameters verification according to the collimators' position (line1: from the start to Col#2, line2: from Col#2 to the coupling point; Gantry: from coupling point to iso center).

The optical parameters of line1 and line2 based on BDSIM-model bear almost no difference from the previous optical design, and the transmission efficiency (line1: 100%, line2: 95.8%) satisfy the design requirements of $\geq 95\%$. However, the optical parameters of the gantry section, whose transmission efficiency is 92.4% ($\leq 95\%$) and isn't capable of meeting expectations, exhibit some dissimilarities from the previous design, as illustrated in Fig. 2.

From Fig. 2, it can be seen that after the beam enters the first dipole, its x-direction envelope is too large, causing its peripheral particles to hit the beam pipe, thus leading to beam loss, which is the reason why the β_x calculated by BDSIM is small than that calculated by MAD-X codes [6].

Therefore, it is necessary to optimize the transmission efficiency of the gantry section. Based on the above analysis,

CALIBRATION EXPERIMENT OF EQUIVALENT AREA OF INDUCTION COIL FOR MAGNETIC FIELD MEASUREMENT OF SUPERCONDUCTING CYCLOTRON

X. Chen[†], S. An, T. Bian, L. Ling, J. Lu, F. Wang, China Institute of Atomic Energy, Beijing, China

Abstract

China Institute of Atomic Energy's 250MeV superconducting cyclotron (CYCIAE-250) uses the induction coil method to measure the magnetic field in its airgap. To ensure the precision of magnetic field measurement, area of the induction coil needs to be calibrated. This paper designs a set of coil calibration technique based on flipping coil method. The uniform magnetic field needed for calibration is provided by a permanent magnet with good static performance, its field is measured through high-precision nuclear magnetic resonance (NMR) probe. Then the induction coil will then be installed at the same position of the NMR probe. During the calibration process, induction coil is rotated 180 degrees and magnetic flux through it will be recorded by a high-speed digital integrator. Corresponding equipment is also designed to finish this task. This Paper describes this magnetic field measurement method, corresponding magnetic measurement equipment, calibration process of the induction coil and calibrated area of the coil.

BACKGROUND

Magnetic Field measurement and shimming is one essential part of cyclotron. There are three main methods of field measurement: hall probe, induction coil and nuclear magnetic resonance [1]. China Institute of Atomic Energy's 250MeV superconducting cyclotron (CYCIAE-250), uses induction coil as field measurement device, which requires the precise area of induction coil.

Calibration method for induction coils used in CYCIAE-230 and other cyclotrons only considers the start point and end point of voltage integral data and can be influenced by nonlinear noise [2-5]. To improve the accuracy of calibration, this article designs a new calibration method and equipment, and then describes the calibration result of the equivalent area of induction coil used for CYCIAE-250.

CALIBRATION METHOD

According to Faraday law of electromagnetic induction, change of magnetic flux through a close circuit will create an induced electromotive force (EMF), of which the amplitude is proportional to the change rate of magnetic flux and the winding number of the circuit:

$$E = -n \cdot \frac{d\Phi}{dt} = -n \cdot \frac{d}{dt} \int \vec{B} \cdot d\vec{S} \quad (1)$$

[†] email address: 962180915@qq.com

The induction coil used for CYCIAE-250 has a small radius and a large winding number, and is connected to digital integrator with twisted pair. The resistance or induction coil and twisted pair's resistance can be neglected, thus the relation between Voltage on the integrator and field through the coil can be described as:

$$V = E = -nS \cdot \frac{dB}{dt} \quad (2)$$

$$B = -\frac{1}{nS} \int V \cdot dt \quad (3)$$

According to Eq. (3), difference of magnet field between two points in the magnetic field can be calculated by recording the voltage produced by induction coil with fast digital integrator. Accordingly, by changing the magnetic field through the coil at a given amount, the equivalent area of coil can be calibrated according to following equation:

$$nS = \frac{1}{\Delta B} \left| \int_{t_1}^{t_2} V \cdot dt \right| \quad (4)$$

Clearing up Linear Drift

When using digital integrator to record induction voltage and its integral value, drift caused by electrical noise must be cleared up [2, 4, 5]. High order cumulant of noise tend to be cancelled out after integration and can be neglected, only the average value of noise voltage will cause a linear drift to the integration result. As a result, real value of coil's equivalent area can be described as:

$$nS = \frac{1}{\Delta B} \left| \int_{t_1}^{t_2} V \cdot dt - V_{off} \cdot T \right| \quad (5)$$

Among the expression, nS is equivalent area of coil, V_{off} is the average value of noise, and T is the integration time.

Calibration Method

A permanent magnet is used to create a constant uniform magnetic field needed for calibration, together with a set of positioning equipment to locate the coil at the centre of magnetic field. First step of calibration is to calibrate the field of permanent magnet with nuclear magnetic resonance (NMR) probe.

NMR probe measures magnetic field through the coupling of hydrogen's nuclear spin (proton spin) and external magnetic field. When applying a external magnetic field, proton spin will precess in the direction of magnetic field. Protons absorb electromagnetic waves at precession frequency and become excited, creating a loss

THE DESIGN OF NONLINEAR REGENERATIVE EXTRACTION IN 250MeV PROTON SUPERCONDUCTING SYNCHROCYCLOTRON

Pengtai Lin, Yufei Yang, XinMiao Wan, Zhiqiang Ren, Wenlong Liao, Xiaobao Luo, Zhihui Li[†],
The Key Laboratory of Radiation Physics and Technology of Ministry of Education, Institute of
Nuclear Science and Technology, Sichuan University, Chengdu, China

Abstract

The objective of this article is to apply the regenerative extraction system to a 250MeV proton superconducting synchrocyclotron. The parameters of the regenerative extraction system are determined by iteratively calculating the appropriate magnetic field and particle trajectory in the region where the magnetic field and particle trajectories interact. This is then combined with the magnetic channel system to achieve the extraction of the beam from the accelerator. In the article, the particle orbit dynamics analysis and the design of relevant parameters for the regenerative extraction system were successfully implemented using Matlab programming. The simulation results showed that the stability in the vertical direction has the greatest impact on the extraction efficiency and determination of the regenerative magnetic field parameters. In order to maximize the particle extraction efficiency, the radial displacement of particles in the last few turns should pass through two identical nodes.

INTRODUCTION

Proton therapy is an effective treatment for cancer with minimal side effects. In recent years, due to the development of superconducting technology, superconducting synchrocyclotron has compact structure and low design difficulty to meet the needs of medical treatment of cancer. The extraction problem is very important in the design process of superconducting synchrocyclotron, and the common extraction methods include electromagnetic deflection system, target scattering beam and regenerative extraction system [1]. The electromagnetic deflection system utilizes deflecting plates to apply a radial electric field force on particles, causing an increase in their orbit radius. The electromagnetic deflection system is suitable for accelerators with large particle orbit spacing, and the particle orbit spacing in the superconducting synchrocyclotron is small, so the application of the electromagnetic deflection system in the superconducting synchrocyclotron will cause some particles to hit the deflection plate and cause unnecessary losses. The target scattering beam method involves scattering the beam into a magnetic channel using a material with a high atomic number. However, this method generally exhibits low extraction efficiency. The regenerative excitation system generates the required magnetic field by adding iron blocks between the edges of the magnetic poles. The generated magnetic field disturbs the particles and causes an increase in their radial amplitude while maintaining stable operation in the vertical direction, thereby

[†] lizhihui@scu.edu.cn.

achieving the goal of extracting particles from the accelerator [2]. The extraction efficiency of the regenerative excitation system can reach between 50% and 70%, indicating a high level of extraction efficiency. In order to promote the development of proton therapy in China, the Key Laboratory of Radiation Physics and Technology, Ministry of Education, has designed an extraction system for a 250MeV proton superconducting synchrocyclotron. The main parameters of the accelerator are shown in Table 1.

Table 1: The Main Parameters of 250MeV Superconducting Synchrocyclotron

Extraction beam energy	250MeV
Magnetic pole radius	53cm
Central magnetic field	5.57T
Ampere-Turn Number	533A-3000turns
RF Cavity Voltage	20kv
RF frequency ranges	58-85MHz

The regenerative extraction system was initially proposed by Tuck and Teng [2] and further improved by Le Couteur [3,4]. The initial regenerative system is linear regeneration, which is a method of increasing the number of "peeler" and the "regenerator" two local magnetic fields on the magnetic pole edge. As shown in Figure 1 (a), these two local magnetic fields are reduced and increased by linear methods in a linear way. Then the study found that only a single increase in the magnetic pole edge of the magnetic pole could also achieve the resulting effect. As shown in figure 1 (b), where the magnetic field of "regenerator" increases nonlinearly with the radius, the magnetic pole utilization rate of this method is higher.

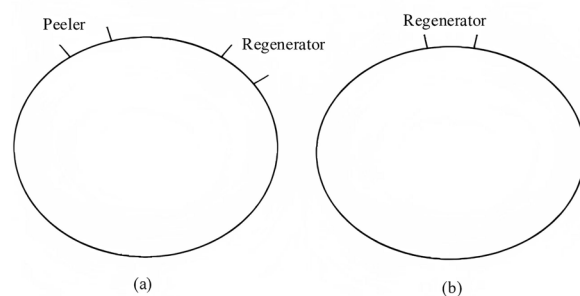


Figure 1: (a) is schematic diagram of linear regenerator extraction, (b) is schematic diagram of nonlinear regenerator extraction.

Appropriate regenerative magnetic field parameters can result in a rapid increase in the radial amplitude of particles while maintaining stability in the vertical direction. When

BEAM DYNAMICS IN SUPERCONDUCTING PROTON LINAC*

Xin-Miao Wan, Yu-Fei Yang, Zhi-Qiang Ren, Peng-Tai Lin, Wen-Long Liao, Xiao-Bao Luo,
Xue-Jiang Pu, Zhi-Hui Li[†]

The Key Laboratory of Radiation Physics and Technology of Ministry of Education, Institute of Nuclear Science and Technology, Sichuan University, Chengdu 610065, China.

Abstract

Beam loss control is a crucial research direction in high-current superconducting linear accelerators (SCL). The research findings include firstly, for continuous beams, when tune depression (η) > 0.7 , zero current periodic phase advance (σ_{0t}) can partially exceed 90° during transport in solenoid and quadrupole doublet periodic focusing channels. Different results occur when $\eta < 0.7$. Secondly, in the solenoid system, σ_{0t} can partially exceed 90° without significant impact on beam quality. In the quadrupole doublet focusing system, the partial breakdown of 90° affects beam quality. Thirdly, Similar conclusions hold for acceleration effects. Fourthly, numerical analysis shows that double-period structures have more stringent design criteria than fully period structures. The double-period structure can cause envelope instability even if $\sigma_{0t} < 90^\circ$. Fifthly, the primary factor causing halo is the 2:1 resonance. Additionally, when η is small, higher-order resonances can also cause halo.

INTRODUCTION

Countries around the world have initiated a series of research projects related to high-power proton superconducting linear accelerators (APT, SNS, J-PARC, CADS, etc.) [1]. The understanding of beam dynamics in high-current SCL has been deepened, leading to the discovery of theories that affect the stability of beam, including envelope instability and particle-core resonance. These findings have been summarized and formulated into a set of fundamental principles for the design of SCL [2]. These principles include ensuring that the σ_{0t} is less than 90° to avoid envelope instability and prevent beam loss [3]. The first principle aims to mitigate envelope instability, while the second principle is derived from studies on halo [4]. In addition, we need to conduct systematic research on the effects of σ_{0t} exceeding 90° in the quasi-periodic focusing structure of the front section of the first acceleration stage in the SCL, as well as the halo in the double-period structure of the cryomodule with a cryostat as a unit [5].

ENVELOPE INSTABILITY

Based on the transverse motion equation, the RF electromagnetic field at the low-energy end of the linear accelerator exhibits defocusing and axial symmetry. In this study, we used a solenoid (with axial symmetry) and a non-axisymmetric quadrupole doublet as the focusing elements.

The specific parameters of these elements are shown in Fig. 1 for reference in the subsequent discussion.

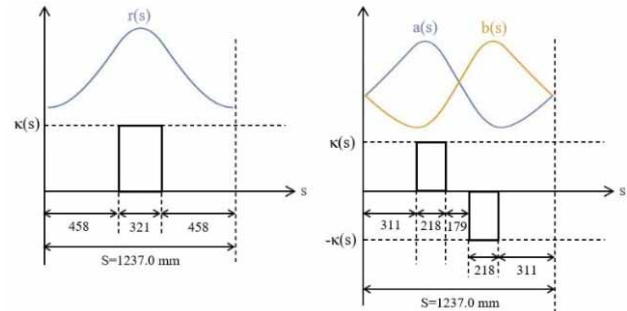


Figure 1: Periodic focusing elements and the corresponding matched beam envelopes. (a) solenoid, (b) quadrupole doublet.

We used *TraceWin* for our simulation and PARTRAN for multi-particle simulation and tracking. The K-V distribution and K-V envelope equations were selected for their advantages in analysing the effect of space charge. The initial kinetic energy of the proton beam was 10 MeV, and the initial normalized RMS emittance of the CW beam was $0.2 \pi \cdot \text{mm} \cdot \text{mrad}$ in both the $x-x'$ and $y-y'$ planes. A total of 100,000 particles were simulated. The envelopes where $X(s)$ and $Y(s)$ are in the two transverse directions of the periodic focusing channels are described by [6]:

$$X'' + \kappa_x(s) \cdot X - \frac{\varepsilon^2}{X^3} - \frac{2K}{X+Y} = 0 \quad (1)$$

$$Y'' + \kappa_y(s) \cdot Y - \frac{\varepsilon^2}{Y^3} - \frac{2K}{X+Y} = 0 \quad (2)$$

To study the transverse beam dynamics when σ_{0t} partially exceeds 90° , we designed five different focusing schemes for simulating σ_{0t} , as shown in Fig. 2. The maximum σ_{0t} of the beam was set to be 120° (①), 110° (②), 100° (③), and 90° (④) to observe the trend under different acceleration gradients in the presence of an acceleration field. To avoid excessive sensitivity to the focusing parameters, we generally set the minimum value of σ_{0t} to 40° after the beam passes through 80 focusing periods. Furthermore, for the case where the maximum σ_{0t} was 120° , we implemented a control scheme (⑤) to prevent envelope instability in the beam. The maximum σ_{0t} of this control scheme was set to 88° , achieved by reducing the acceleration gradient of the corresponding cavity.

* Work supported by the National Natural Science Foundation of China (Grant Nos. 11375122 and 11875197)

[†] lizhahui@scu.edu.cn

THE DESIGN OF A PROTON-HEAVY ION HYBRID SYNCHROTRON UPGRADED FROM XIPAF PROTON RING

H. J. Yao^{1,2,3}, X. Y. Liu^{1,2,3}, Y. Li^{1,2,3}, Z. J. Wang^{1,2,3}, S. X. Zheng^{1,2,3†}, X. W. Wang^{1,2,3}, Z. M. Wang⁴

¹Key Laboratory of Particle & Radiation Imaging (Tsinghua University), Ministry of Education, Beijing, China

²Laboratory for Advanced Radiation Sources and Application, Tsinghua University, Beijing, China

³Department of Engineering Physics, Tsinghua University, Beijing, China

⁴State Key Laboratory of Intense Pulsed Radiation Simulation and Effect (Northwest Institute of Nuclear Technology), Xi'an, China

Abstract

Xi'an 200 MeV Proton Application Facility (XiPAF) has been basically completed at the end of 2020, providing proton beams of 10 to 200 MeV for space radiation effect studies on electronics. To expand its capabilities, XiPAF is undergoing an upgrade to deliver multiple ion species, from proton to Bismuth ion. The upgrade focuses on three aspects. First, the original negative hydrogen linear injector will be remodelled to a proton linac injector. Second, a heavy ion linear injector will be added. Third, the existing proton ring will be retrofitted into a hybrid proton-heavy ion synchrotron. This paper details the considerations and physical designs for upgrading the synchrotron. Within the scope, we discuss the challenges and solutions in transforming a specialized proton synchrotron into a multi-ion accelerator under the constraints of existing plant layout and reuse of existing equipment.

INTRODUCTION

XiPAF is a dedicated facility for space radiation environment simulation. It has been designed since 2014, and the beam commissioning was completed in a temporary plant at the end of 2020 [1], providing 10 ~ 200 MeV proton beams for irradiation experiments, while the formal plant is also under construction. With the continuous development of space radiation effect studies, new demands have been put forward for the device. Therefore, the XiPAF-Upgrading project was proposed and approved. The requirements and basic principles of XiPAF-Upgrading are:

- Expanding ion species from protons to multiple ions containing protons and heavy ions.
- The size of the upgraded accelerator complex is required to be within the layout of the plant under construction.
- Reuse the original equipment of XiPAF as much as possible to reduce costs.

XiPAF-Upgrading project began design in 2022 and beam commissioning is scheduled to be completed by the end of 2025. The overall layout of XiPAF-Upgrading is shown in Fig. 1. The original H⁻ linac injector of XiPAF will be changed to H⁺ injector with an energy of 7 MeV. A set of heavy-ion linac injector will be added, the charge-to-mass ratio range of the heavy ions to be accelerated is

1/2~1/6.5, and the energy is 2 MeV/u. The original proton ring will be upgraded to a proton-heavy ion hybrid synchrotron, and two terminals are for proton and heavy ion experiments respectively.

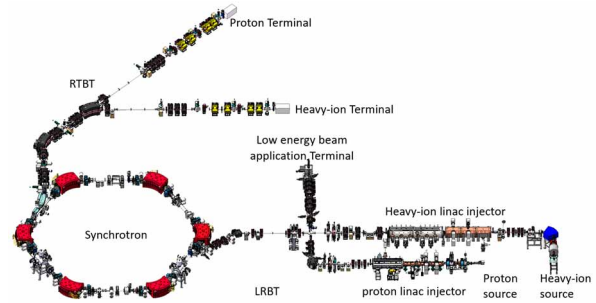


Figure 1: The overall layout of XiPAF-Upgrading.

The main parameter requirements of XiPAF-Upgrading synchrotron are shown in Table 1. The existing equipment needs to be reused, and the size of the synchrotron is limited by the size of the plant (ring circumference ≤ 40 m). Under these constraints, the physical design of the proton-heavy ion hybrid synchrotron upgraded from a proton ring is reported.

Table 1: Design Requirements of XiPAF-Upgrading Synchrotron

Ion	Injection Energy [MeV/u]	Extraction Energy [MeV/u]	Particle No. [ppp]
H ⁺	7	10~200	1×10 ¹⁰
He ⁺	2	4	1×10 ⁸
C ⁴⁺	2	9	1×10 ⁸
Si ⁸⁺	2	7	1×10 ⁷
Ar ¹¹⁺	2	4	1×10 ⁷
Kr ¹⁸⁺	2	6	1×10 ⁷
Bi ³²⁺	2	6	1×10 ⁷

LATTICE DESIGN

To upgrade XiPAF proton ring to a proton-heavy ion hybrid synchrotron, two major issues need to be addressed: (1) vacuum; (2) injection. To meet the requirements of the heavy-ion beam lifetime, the vacuum pressure of the synchrotron needs to be upgraded from 1×10^{-6} Pa to 5×10^{-10} Pa. XiPAF proton ring adopts the H⁻ stripping injection, to

† zhengsx@tsinghua.edu.cn

ELECTRON COOLING FOR FUTURE HIGH-ENERGY HADRON ACCELERATORS*

H. Zhao[†]

Institute of Modern Physics, CAS, Lanzhou 730000, China

Abstract

Electron cooling is an important method to reduce the emittance and momentum spread of hadron beams, and it has been successfully applied in several facilities around the world. In 2019, the world's first RF-based electron cooler (LEReC) was commissioned at BNL for the RHIC BES-II project, and the integrated luminosity of RHIC is finally doubled. In addition, electron cooling is also a must for the future Electron-Ion Collider (BNL EIC). However, the high energy requirement of the electron beam (150 MeV) is far beyond what all present coolers can achieve (<4.3 MeV). For that, an electron ring cooler with strong radiation damping is proposed and designed, in which the non-magnetized and dispersive cooling techniques are applied. In this paper, I will introduce the physical design and some important considerations of the ring cooler.

INTRODUCTION

Electron cooling is a powerful method to shrink the size and momentum spread of the stored ion beams for accumulation and high-precision experiments. Since it was first proposed by G. I. Budker in 1967, this technique has been widely applied and developed in many heavy ion accelerators around the world [1, 2]. With the development of particle accelerators and the higher requirements for experimental physics, beam cooling with much higher energy electron beam is demanded.

Up to now, all electron coolers built around the world are based on dc electron beams, which are accelerated by electrostatic fields. The highest-energy electron cooling system with 4.3 MeV electrons has been successfully constructed and operated at Fermi National Accelerator Laboratory in 2005 [3]. Recently, the world's first rf-based electron cooler is successfully commissioned at BNL and the cooling of gold beams in RHIC by 1.6 MeV and 2.0 MeV electron was successfully achieved [4]. It provides the possibility to use similar approach to develop high-energy electron coolers in the future.

Brookhaven National Laboratory (BNL) is designing an Electron-Ion Collider (EIC), which will be a new discovery machine that opens new frontiers for the researches in nuclear physics and quantum chromodynamics [5]. In order to maintain the high luminosity during long collision runs, it is desirable to cool the hadron beam (275 GeV proton) to counteract the emittance growth caused by intrabeam scattering (IBS) [6]. However, the conventional coolers and the

rf-based coolers are no longer suitable for such high energy beam cooling in EIC. In fact, various proposals and new cooling schemes have been proposed, but the technical and experimental demonstrations are still lacking. In this paper, we present a design of electron storage ring cooler with bunched electron beam for the EIC [7].

EIC COOLING DEMANDS

For the EIC, the most demanding case is to cool the proton beam at the energy of 275 GeV. During the long collision stores, the emittance growth of proton beam due to IBS is the dominant limitation for the luminosity. The requirement for the hadron beam cooling is mainly to counteract the IBS heating effect. The evolution of the 275 GeV proton beam emittance caused by IBS is shown in Fig. 1. It shows that the IBS heating effect for the flattened proton beam is dominated by the horizontal and longitudinal planes. As a result, vertical cooling is not needed for EIC. So, one can effectively use horizontal dispersion to redistribute the cooling rates between the longitudinal and horizontal planes, and achieve required cooling performance.

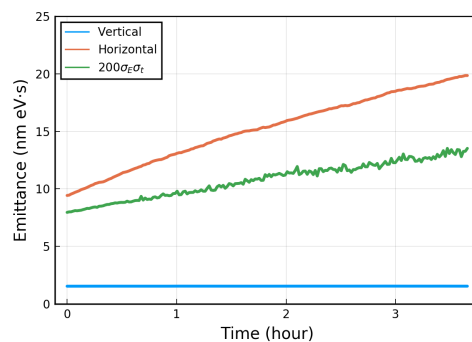


Figure 1: Emittance growth of the 275 GeV proton beam caused by IBS in EIC.

RING COOLER DESIGN

Overview

The electron storage ring has a race track shape, with the cooling section located in one long straight section and wigglers in the other. The ring is mirror symmetric around the center of the cooling section, and the top view of the ring is shown in Fig. 2. The cooling section has a length of 170 m and it fits into the straight section of the hadron ring. There are four arcs with radius of 3.42 m, each of them has 10 dipoles and a 90 degree phase advance per cell. The wiggler section is also mirror symmetric with four pairs of wigglers in each half. In our setup, the alternating horizontal and

* Work supported by the National Natural Science Foundation of China (No. 12275323)

[†] hezhao@impcas.ac.cn

INFLUENCE OF TRANSVERSE DISTRIBUTION OF ELECTRON BEAM ON THE DISTRIBUTION OF PROTON BEAM IN THE PROCESS OF ELECTRON COOLING*

Xiaodong Yang[†], Institute of Modern Physics, CAS, Lanzhou, China

Abstract

The electron cooling process of 20 GeV proton beam in EicC was simulated for the eight transverse distribution of electron beam with the help of electron cooling simulation code. The transverse cooling time was obtained in the different transverse distribution of electron beam. The final transverse distribution of proton beam was demonstrated. The simulated results reveal that the transverse distribution of electron beam influences the distribution of proton beam in the process of electron cooling. In the future, this idea was expected to apply to the longitudinal distribution of electron beam. The longitudinal distribution of proton beam was attempted to be controlled by the longitudinally modulated electron beam. As a result, the peak current and longitudinal distribution of proton beam will be controlled by the electron beam. The loss of proton beams will be reduced, and the stored lifetime of proton beam in the storage ring will be extended. The intensity of the proton beam will be maintained for a longer time.

INTRODUCTION

The electron cooling process of 20 GeV proton beam in EicC was simulated in cases of variety of parameters [1].

The transverse electron cooling time [2] not only depends on the lattice parameters of the storage ring, the Betatron function, dispersion of the cooling section, such as energy, initial emittance and momentum spread of proton beam, but also on the construction parameters of electron cooling device, the strength of magnetic field, the parallelism of magnetic field in the cooling section, the effective cooling length, and the parameters of electron beam, such as radius, density and transverse temperature of electron beam. These parameters are determined by the storage ring and the technology limitation, on the other hand, they are influenced and restricted each other.

As mentioned in the reference [3, 4], As a result of electron cooling, the core of beam distribution is cooled much faster than the tails, producing a denser core. To account for a core collapse of ion distribution. The core directly impacts luminosity in a collider.

From the experiments results from LEReC BNL [5], Application of electron cooling directly at the collision energy of the hadron beams brings some challenges. Of special concern is control of the ion beam distribution under cooling in order not to overcool the beam core. As a result, most of the ions experienced linear part of the friction force without overcooling of ion beam distribution. Providing

transverse cooling appeared to be more beneficial for collider operations compared to the longitudinal cooling. This is because longitudinal cooling led to higher peak currents of ions, affecting the ion beam's lifetime due to the space-charge effects.

MOTIVATION

High intensity proton beam and short bunch length was expected to store in a collider with long lifetime and less loss. In order to increase the lifetime of proton beam and decrease the loss, longitudinally modulated electron beam [6, 7] will be attempted to suppress the intra-beam scattering. The traditional DC electron beam in the electron cooler will be modulated into shorter electron bunch with different longitudinal distribution. The stronger cooling was expected in the tail of proton beam and the weaker cooling was performed in the core of proton beam. The proton loss will be decreased and the lifetime will be increased. The intensity of proton beam in the collider will be kept and maintained for longer time.

ELECTRON BEAM DISTRIBUTION

The distribution of electron beam was uniform in the transverse direction in the traditional simulation of electron cooling. The electron density was uniform in the radial direction.

In order to investigate the influence of transverse distribution of electron beam on the distribution of ion beam in the process of electron cooling, eight kinds of electron beam profiles were attempted in the simulation shown in Fig. 1.

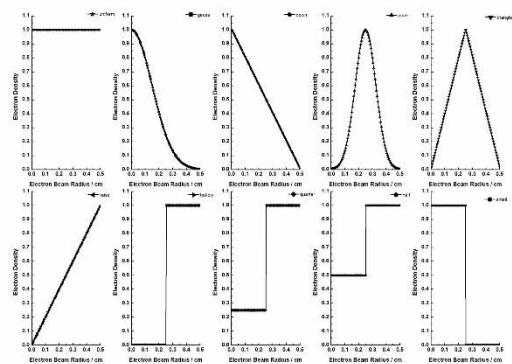


Figure 1: The transverse distribution of electron beam.

Due to the distribution of electron beam in the transverse direction was axial symmetry, only half distribution was described in the simulation.

* Work supported by NSFC No. 12275325, 12275323, 12205346.

[†] email address yangxd@impcas.ac.cn.

DESIGN OF A SYNCHROTRON FOR PROTON FLASH RADIOTHERAPY BASED ON FAST VARIABLE-ENERGY BUNCH SPLITTING*

Y. Li, H. J. Yao, S. X. Zheng[†], Q. Z. Xing[‡], X. W. Wang

Key Laboratory of Particle & Radiation Imaging, Ministry of Education, Beijing, China

[†]also at Laboratory for Advanced Radiation Sources and Application,
Tsinghua University, Beijing, China

[‡]also at Department of Engineering Physics, Tsinghua University, Beijing, China

Abstract

Ultra-high dose rate (FLASH) radiotherapy not only guarantees effective tumor treatment but also greatly enhances the protection of normal tissue. Moreover, it is a convenient procedure for tumor patients that has enhanced the benefits provided by medical institutions. Proton FLASH radiotherapy, which combines the Bragg peak effect of proton spatial dose distribution with the unique temporal effect advantage of FLASH, is an attractive tumor treatment approach. To achieve proton FLASH discrete pencil beam scanning in a 1-L volume, taking into account the 5-mm point interval, 9261 points would need to be irradiated within 500 ms, which is beyond the capability of existing medical devices. To meet these requirements, based on a fast cycle synchrotron with a period of 25 Hz, we simultaneously combined variable-energy, fast splitting, and extraction beam bunches, and proposed a scanning method suitable for continuous variable-energy extraction bunches. The proposed technique meet the requirements of proton FLASH discrete pencil beam scanning within a volume of 1 L.

INTRODUCTION

While ensuring the effect of tumor treatment, FLASH therapy greatly reduces the damage to normal tissue cells [1], and at the same time brings convenience to tumor patients and improves the benefits of medical institutions. Proton FLASH therapy, which combines the Bragg peak effect advantage of spatial dose distribution and the unique time effect advantage of FLASH therapy, is a very attractive tumor therapy. The ultra-high dose rate (>40 Gy/s) and very short treatment time (usually less than 500 ms) in the target area of FLASH therapy impose high requirements on the accelerator outlet beam intensity and energy transformation time. Synchrotron has the advantage of active energy regulation. Using proton synchrotron in FLASH therapy combined with spot scanning irradiation therapy with high beam utilization rate is expected to meet the requirements of dose rate and irradiation time in the target area.

Due to the high requirements of proton FLASH therapy for dose rate and treatment time, only some medical institutions have conducted proton radiotherapy based on small

volume or fixed energy penetration irradiation on cyclotrons. Some preliminary results of these experiments have shown the effect of FLASH therapy, but further research is needed in more functional proton radiotherapy equipment. At present, cyclotrons are mainly used in medical institutions around the world. However, cyclotrons have low energy regulation speed, high beam loss and great influence on beam quality, which is not conducive to the treatment of tumors with large depth distribution. Synchrotron has the advantage of active energy regulation, which can shorten the energy regulation speed and ensure the beam quality, and has certain advantages in the application of FLASH therapy. However, some key problems still need to be solved in the application of proton synchrotron in FLASH therapy.

KEY ISSUES AND CHALLENGES

Proton FLASH therapy is a kind of ultra-high dose rate radiotherapy. The average dose rate is not less than 40 Gy/s and the total irradiation time is in the order of hundred milliseconds. For the pencil beam scanning method, the average dose rate in the target scanning process can be calculated according to the dose sum of each scanning point and the total scanning time:

$$\dot{D} = \frac{D}{T} = \frac{\sum_{i=1}^n D_i}{\sum_{i=1}^n (T_{del,i} + T_{scan,i}) + \sum_{j=1}^m T_{energyswitch,j}} \quad (1)$$

where, \dot{D} is the dose rate; D is the dose sum of each scanning point; T is the total treatment time; there are n scanning points and m energy switching processes; D_i is the dose of each scanning point; $T_{del,i}$ and $T_{scan,i}$ are the beam delivery time and scanning time of each scanning point, respectively; and $T_{energyswitch,i}$ is the time of each energy switching.

To improve the average dose rate, it is necessary to increase the number of particles reaching the target area during the treatment time, and to shorten the delivery time, energy switching time, and scanning time. In the volume of 1 L, to meet the minimum dose rate requirement of 40 Gy/s for proton flash therapy, the number of particles required for 100 ms was 3.8×10^{11} [2].

At present, medical institutions providing radiation therapy around the world mostly use cyclotrons to extract beams of fixed energy, and irradiate in the target area after energy regulation. Energy regulation with a range shifter

* Work supported by National Natural Science Foundation of China (No. 12075131).

[†] zhengsx@tsinghua.edu.cn

[‡] xqz@tsinghua.edu.cn

NEW PROGRESS OF THE MINIATURIZED MICROWAVE ION SOURCE AT PEKING UNIVERSITY*

S. X. Peng^{1, †}, T. H. Ma¹, W. B. Wu¹, B. J. Cui¹, A. L. Zhang², Y. X. Jiang¹, Z. Y. Guo¹, J. E. Chen¹

¹State Key Laboratory of Nuclear Physics and Technology & Institute of Heavy Ion Physics, Peking University, Beijing, China

²State Key Laboratory of Particle Detection and Electronics, Department of Modern Physics, University of Science and Technology of China, Hefei 230026, China

Abstract

The generation of plasma in a microwave ion source involves confining electrons using a static magnetic field and energizing them with an electromagnetic field that transmitted into the plasma chamber. However, according to electromagnetics theory, there is always a cut-off size in circular wave guides for a given frequency. For a 2.45 GHz microwave, this dimension is 72 mm, which should theoretically prevent transmission of the microwave into the discharge chamber and no plasma can be generated. Since 2006 Peking University (PKU) has successfully developed a series of permanent magnet 2.45 GHz microwave ion sources (PKU PMECRs) with a discharge chamber less than 50 mm, capable of delivering tens of mA beams for accelerators. To explain this anomalous phenomenon, a hybrid discharge heating (HDH) mode that combines surface wave plasma (SWP) and electron cyclotron heating (ECH) has been proposed. This HDH mode not only successfully explains PKU PMECRs, but also predicts that the optimized inner diameter of the plasma chamber is 24 mm, which is confirmed by experiments involving different liners in the miniaturized microwave ion source.

INTRODUCTION

Microwave ion sources (MISs) operating at 2.45 GHz have found widespread use in scientific research, industry, agriculture, and medical science due to their high intensity, low emittance, high stability, simple structure, low cost, and long lifetime [1]. For example, tens even hundred milliamperes H⁺, D⁺, etc. ion beams have been obtained by 2.45 GHz ECR sources, such as CEA/Saclay, PKU [2][3]. Their rms emittance is about 0.2 π -mm-mrad. Through long term operation test, CEA/Saclay has made a record with 103 hours CW beam operation with no spark or plasma fault occurred in 2001. In 2016, PKU group improved this non-spark record up to 300 hours. Up to now, no new long term CW beam operation result can be found in the world.

Recently, there has been growing interest in high current miniaturized microwave ion sources (MMISs) for use in compact equipment such as neutron generators, ion thrusters, and ion implanters [4-6]. Despite impressive performance exhibited by MMISs generating overdense plasma ($n > 10 n_{\text{cutoff}}$) over the past few decades [7,8], theoretical

studies on the breakdown mechanism of MMISs remain perplexing. Conventional microwave transmission theory suggests that the chamber diameter of a 2.45 GHz MIS should be larger than the cutoff size of a 2.45 GHz microwave [9], implying that microwaves cannot penetrate into the plasma chamber of MMISs with a diameter smaller than 72 mm.

In our previous work, a novel HDH mode is put forward to understand the complex mechanism of the MMISs [10]. The HDH mode believes that the initial stage of plasma establishment is based on SWPs and the plasma maintenance is based on ECH. In this paper, we will present the HDH mode in details. Meanwhile, the optimized inner diameter of the plasma chamber will be investigated systematically.

THE MINIATURIZED MICROWAVE ION SOURCE

The MMIS of PKU is composed of microwave window, plasma chamber, permanent magnet rings, and extraction system. A schematic diagram of the source body of the MMIS is presented in Figure 1. The 2.45 GHz microwave of TEM mode produced by microwave generator is transmitted through coaxial line, then transformed to TE₁₀ mode in the coaxial-waveguide transition by a N-type connector and transformed to TE₁₁ mode in circular microwave window and finally injected into the plasma chamber. The microwave window is composed of 3 alumina layers with the diameter of 27 mm. A piece of BN is placed behind the microwave window, which faces plasma to protect the alumina from the backbombed electrons. The dimension of plasma chamber is $\Phi 30$ mm \times 40 mm. The mirror magnetic field is produced by a set of permanent magnets surrounded plasma chamber. The diameter of the chamber can be changed by inserting liners with different inner diameters. In addition, three NdFeB permanent magnet rings are installed around the plasma chamber to provide a magnetic field for the plasma confinement. The magnetic field distribution is presented in Figure 2, it can be found that the axial magnetic field is a magnetic-mirror field with $B_{\text{max}} > 875$ Gs. A 50 kV three-electrode extraction system consisting of a plasma electrode, suppressor electrode and ground electrode is used for beam extraction.

* Work supported by the National Natural Science Foundation of China (Grant Nos. 12205019, 12147144, and 11975036).

[†] sxpeng@pku.edu.cn

WAKEFIELD STUDIES FOR THE STEP STRUCTURE AND THE SKIN DEPTH OF COATED DIELECTRIC TUBES

H. Liu^{†1}, Shanghai Institute of Applied Physics, Chinese Academy of Sciences Shanghai, China
 J. J. Guo, Zhangjiang Laboratory, Shanghai, China
 Y. M. Wen, S. Chen, B. Liu, H. X. Deng,
 Shanghai Advanced Research Institute Chinese Academy of Sciences, Shanghai, China
¹also at Shanghai Advanced Research Institute Chinese Academy of Sciences, Shanghai, China

Abstract

Wakefield issues are always important in free electron laser (FEL) facilities. Since the wakefield in free electron laser facilities usually leads to a decrease of FEL performance, the research of the wakefield impacts is of great significance. Step structures are almost ubiquitous in the overall undulator section of an FEL facility, which always generate critical wakefields. In this paper, we systematically analyse and summarize the wakefield characteristics of step structures including the step-in and the step-out. In addition, the skin depth issue of the wakefield is still controversial. We study the skin depth of the wakefield field in the vacuum chamber of the kicker in the Shanghai high-repetition-rate XFEL and extreme light facility (SHINE), which is made of the dielectric tube. We proposed the conception of “effective skin depth” from two different perspectives and wrote simulation codes to calculate the “effective skin depth”. We hope these methods could provide new mentalities for related research in the future.

INTRODUCTION

FEL lasing performance largely depends on the quality of electron bunches [1]. While the wakefield generated by the electron bunch always destroys its phase space, which leads to a decrease of lasing performance [2-4]. Since there are many different types of devices the inner apertures of chambers in different devices are always different. The connection of chambers with different apertures is called step structure. In our research before [5, 6], we found that the wakefield generated in step structures is an important component of the total wakefield of an FEL facility. The step structure wakefield even contributes half of the total wakefield. Therefore, the study of the step structure wakefield is important for FEL. There are currently some studies on the step structure wakefield, but there is still a lack of systematic summary of the characteristics of this kind of wakefield. In this paper, we calculate and analyse the step structure wakefield in different situation and initially list its characteristics comprehensively.

In our study of the wakefield in the kicker of the SHINE, we found that the skin depth issue in wakefield calculations

is still unsolved. Different teams presented different perspectives. In this paper, we proposed the conception of “effective skin depth” from the perspective of the accumulation of free charges and the attenuation of the surface current. We calculate the effective skin depth using our own simulation code. The results demonstrate the feasibility of the development of this conception in the future.

WAKEFIELDS OF THE STEP STRUCTURE

The step structure includes two types of structures, the step-in and the step-out. The former means the structure whose aperture varies from large to small while the latter is the opposite structure to step-in. There are two connection types of step structures, the saltatory type is called the “hard connection” and the “soft connection” means a gradual change of aperture. Although there are some research about the step structure wakefield, some questions are still unsolved. In this section, we will answer these questions based on our simulation results (simulation code: ECHO2D [7]).

Short Bunch Situation

In our research before, we always ignore the effect of step-in wakefield since its value is much smaller than that of step-out wakefield. Taking the situation in the SHINE as an example, we calculated wakefields of a step-in and a step-out with soft (taper) and hard connection schemes. The parameters are listed in Table 1 and the simulation results are shown in Figure 1.

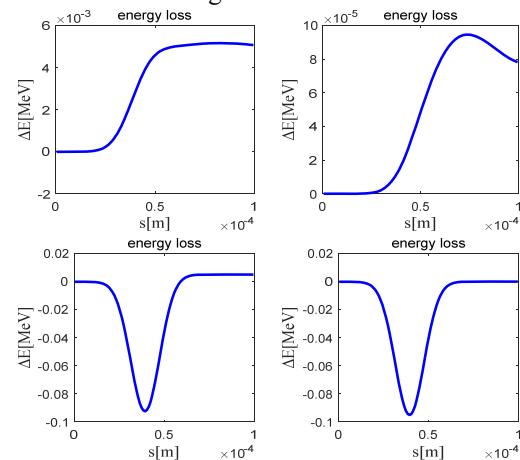


Figure 1: Simulation results of step structure wakefields in short bunch situation.

* Work supported by the CAS Project for Young Scientists in Basic Research (YSBR-042), the National Natural Science Foundation of China (12125508, 11935020), Program of Shanghai Academic/Technology Research Leader (21XD1404100), and Shanghai Pilot Program for Basic Research – Chinese Academy of Sciences, Shanghai Branch (JCYJ-SHFY-2021-010).

[†] email address

liuhe@sairi.ac.cn.

HEATING ESTIMATION OF UNDULATOR VACUUM CHAMBER AT S³FEL

Huaiqian Yi¹, Xiaofan Wang^{1*}, Weiqing Zhang^{1,2†}, Xueming Yang^{1,2,3}

¹Institute of Advanced Science Facilities, Shenzhen 518107, China

²Dalian Institute of Chemical Physics, Dalian 116023, China

³Southern University of Science and Technology, Shenzhen 518055, China

Abstract

Heating of the vacuum chambers are unavoidable when electron beams pass through the chamber channels at relativistic speeds. In the undulator vacuum chambers, such effects might lead to temperature increase of the magnets and eventually cause degradations in the FEL lasing process. Thus, in this paper, the heating of the undulator vacuum chambers at Shenzhen superconducting soft x-ray free-electron laser due to wake field effects and spontaneous synchrotron radiation are estimated using an analytical approach. For the wake field effects, the contribution from finite conductivity of the vacuum chamber material and from the inner surface roughness are considered. An electron beam profile from a start-to-end simulation is used to calculate the total wake field and the induced heat. For the synchrotron radiation, a simple analytical expression is used.

INTRODUCTION

At Shenzhen superconducting soft x-ray free-electron laser (S³FEL) [1], electron beams from the injector system are accelerated in a single superconducting linac and transported to the undulator lines through the beam distribution system (BDS). At the end of the BDS, the typical electron beam parameters are given in Table 1. The maximum designed repetition rate of the electron bunches is 1MHz.

Table 1: Electron Beam Parameters

Beam Parameters	Value	Unit
Electron Energy	2.5	GeV
Slice Energy Spread	190	keV
Electron Bunch Charge	100	pC
Slice Emittance	0.5	mm·mrad
Rms Bunch Length	25	μm

When electron beams pass the vacuum chambers of the beam lines, heat will be deposited in the chamber walls due to electrons losing energy when interacting with their own wake fields.

The heating problems may become prominent for vacuum chambers in the undulators since the chamber transverse dimensions are small compared to other parts along the beam lines, and the wake field effects are stronger. In

addition, spontaneous synchrotron radiation is generated and absorbed by the chamber walls.

The vacuum chambers within the undulators at S³FEL are made of extruded aluminium with an elliptical cross-section, as shown in Fig. 1. The full height and width of the chamber cavity are 6 mm and 15 mm, respectively. The two circular holes adjacent to the chamber are for the water-cooling system, while the two outermost holes are space designed for correction coils.

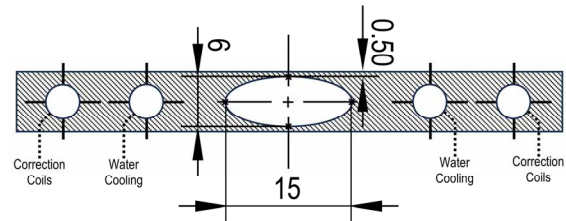


Figure 1: Cross-section of the vacuum chamber geometry.

If excessive heat in the vacuum chambers is not removed efficiently by the cooling system, the temperature gradient within the permanent magnet blocks will be affected and the magnetic field distributions and undulator K values will be modified. This will result in a negative impact on the FEL lasing process.

Under such considerations, the heat load projected on the vacuum chambers by the two heat sources mentioned above is estimated analytically in this paper. The results will serve as supplementary information to aid the design of the cooling system.

WAKE FIELD EFFECTS

The wake fields due to wall resistivity and the roughness of the inner surface of the vacuum chamber are considered in this work. Wake fields generated by single or periodic structures or other effects are ignored. A simplified approach is taken in the current calculations, where the longitudinal distributions of the electron beams is assumed to be unchanged as they travel down the undulator lines.

Calculation of the Wake Fields

The analytical approach first involves the calculation of resistive wall and roughness induced surface impedance and thereafter the longitudinal beam impedance Z . The latter depends on the cross-section shape of the vacuum chamber, and in this work, both round and flat plate

* wangxf@mail.iasf.ac.cn

† weiqingzhang@dicp.ac.cn

RECENT PROGRESS OF THE BEAM BACKGROUND EXPERIMENT IN THE BEPCII*

B. Wang^{†1}, H.Y. Shi¹, H.C. Shi², C.H. Yu¹

¹ Key Laboratory of Particle Acceleration Physics and Technology,
Institute of High Energy Physics, Chinese Academy of Sciences, Beijing, China

² Zhejiang University, Hangzhou 310027, People's Republic of China

Abstract

The Beijing Electron Positron Collider II will upgrade to extend the beam energy and the luminosity by increasing the beam current and slightly compressing the beam size, where the beam energy will be extended from 2.3 GeV to 2.8 GeV and the peak luminosity will be up to $1.1 \times 10^{33} \text{cm}^{-2} \text{s}^{-1}$ at the optimizing beam energy of 2.35 GeV. The BEPCII upgrade is expected to result in challenging levels of beam related background in the interaction region. An precise simulating and mitigating beam background is necessary to protect the BESIII detector and increase the beam current and peak luminosity. The beam related background at BEPCII is mainly from the Touschek effect and the beam gas effect, this paper presents the recent progress of the beam background simulation and experiment.

INTRODUCTION

The Beijing Electron Positron Collider II (BEPCII) [1] is a two-ring electron positron collider which has operated successfully for over 10 years and collected more than 40fb^{-1} data sets in the τ -charm energy range. A series of significant experimental observations have been reported based on these data sets [2]. In 2019, BESIII collaboration has reported the future physics programme (also called “white paper”) which contains a detailed survey of important topics in τ -charm physics and hadron physics [3]. However, the age of BEPCII becomes an important issue, such as main drift chamber (MDC). Due to the beam-induced with a hit rate up to 2kHz/cm^2 , the cell gains of the inner chamber drops dramatically (about 39% drop for the first layer cells in 2017) and furthermore lead to a degradation of the spatial resolution and reconstruction efficiency [3]. In addition, the peak luminosity of BEPCII is optimized at 1.89 GeV, the evaluated peak luminosity at 2.35 GeV is only $0.35 \times 10^{33} \text{cm}^{-2} \text{s}^{-1}$. Therefore, an upgrade is required for BEPCII to collect more data sets in this energy region, especially at center-of-mass energies larger than 4 GeV [4]. The peaking luminosity at 2.35 GeV will increase to $1.1 \times 10^{33} \text{cm}^{-2} \text{s}^{-1}$ with high beam current and small beam size. However, the resulting high beam background must be controlled within a safe range.

In the beginning of BEPCII, ten collimators with fixed aperture were installed on both the electron and positron rings. Three horizontal movable collimators were installed at 8.2 m, 11 m upstream, and 11 m downstream from IP

on the electron ring, and a horizontal movable collimator was installed at 8.2 m upstream from IP on the positron ring. Simulations of beam-gas effect [5], Touschek effect [6], SR [7] and movable collimators [8] were separately studied to predict the background rate in BESIII. These collimators obviously mitigated the beam background and played an important role in the stable operation of the BEPCII machine in its initial stage. Each movable collimator has a pair of movable jaws which is able to adjust their aperture independently. Due to the high beam current and small beam size of BEPCII upgrade project, it is necessary to reexamine beam background simulation and experiments.

BEAM BACKGROUND SIMULATION AND EXPERIMENT IN 2021

The beam background at BEPCII consists of luminosity-related background and beam-related background, where the first one is generated by beam-beam interaction and can be simulated with an acceptable precise, the second one is highly dependent on beam parameters and the storage ring. The dominant sources of beam-related background can be parameterized by:

$$O_{\text{SingleBeam}} = S_{\text{tous}} \cdot \frac{I_t \cdot I_b}{\sigma_x \sigma_y \sigma_z} + S_{\text{gas}} \cdot I_t \cdot P(I_t) + S_{\text{const}}, \quad (1)$$

where $O_{\text{SingleBeam}}$ is the total background rate of single beam and can be described by the dark current or count rate of the machine-detector interface (MDI). The first term (the Touschek background) is proportional to bunch current (I_b) and beam current (I_t), and inversely proportional to beam size ($\sigma_{x,y,z}$). The second term (beam-gas background) is proportional to beam current and vacuum pressure. Generally, the residual gas mainly comes from the interactions between synchrotron radiation (SR) photons and the inner wall of beam pipe, so the vacuum pressure depends on the beam current. The third term is the constant background from cosmic rays and electronic noise, independent of the beam condition and can be presented by a constant term.

The beam-related background simulation is based on the framework which includes generators for lost particles, SAD [9] for tracking the particles in the collider ring, and Geant4 [10] and Geant4-based software framework of the BESIII offline software system (BOSS) [11] for simulating the detector's responses and MDI. The beam background experiment was performed for validating the simulation result. The “data/MC” ratio, which is the ratios of the background

* Work supported by the National Natural Science Foundation of China (NSFC), under Contract No. 11905225

[†] corresponding author: wangbin@ihep.ac.cn